Hydrological Processes

WILEY

RESEARCH ARTICLE OPEN ACCESS

A Multi-Century Meteo-Hydrological Analysis in the Italian Alps: Daily Streamflow (1862–2022) at Different Time Scales

Roberto Ranzi[1] | Emanuele Eccel[2] | Paolo Colosio[1] | Eleni M. Michailidi[1,3]

[1]Department of Civil, Environmental, Architectural Engineering and Mathematics, Università degli Studi di Brescia, Brescia, Italy | [2]Fondazione Edmund Mach, San Michele all'Adige, Italy | [3]Innovation and Development Office, GAIA S.P.A., Pietrasanta, Lucca, Italy

Correspondence: Roberto Ranzi (roberto.ranzi@unibs.it)

Received: 27 April 2025 | **Revised:** 11 October 2025 | **Accepted:** 15 October 2025

Funding: This work was supported by Po River District Basin Authority (Grant Number 8536/2020) and University of Brescia.

Keywords: Adige | Alpine Rivers | attribution science | climate change | streamflow | wavelet spectrum

ABSTRACT

In this paper, the second longest time series of daily hydrometric levels and streamflow for an Italian river, Adige, in the Italian Alps, also one of the longest worldwide and unpublished so far, is reconstructed and analyzed. Daily streamflow prior to 1923, when the official mean daily discharge was first published, is estimated based on daily water levels collected since January 1862, cross-section geometry, discharge, and surface velocity measurements at the hydrometric station of Trento. The main objective of this paper is the identification, attribution, and quantification of the impact of natural and anthropic factors on changes in streamflow in a mountain region with marked orographic and climatic gradients. The resulting 161-year-long time series, until December 2022, for this 9763 km^2 catchment is firstly analyzed in search of trends and their statistical significance, spectral properties at different time scales and periods, changes in the monthly regime prior to and after the constructions of reservoirs. The observed −1.0 mm year^{-1} slope of the annual streamflow linear trendline is statistically significant and indicates a decline of −1.4% per decade of available streamflow in the river, similar to the one observed in nearby basins. The spectral analysis conducted with the wavelet transform indicates that a sudden change of spectral properties and trends of daily streamflow occurred inside the pre- and post-reservoir construction period and can be explained also as a result of a more environment-oriented legislation. A wavelet coherence spectrum between streamflow and teleconnection indices indicates the existence of a significant coherence with the Atlantic Multidecadal Oscillation only. The comparison with estimated actual reference evapotranspiration losses and temperature points out that the observed temperature increase is not sufficient to explain the observed hydrological losses, being precipitation almost constant over the observation period. The observed increase of 86 mm of hydrological losses over the last century is explained in terms of water withdrawals for agricultural, civil, and industrial needs (38 mm), enhanced evapotranspiration due to temperature increase (30 mm), expanded artificial lakes' surface (1 mm), the residual of 17 mm being attributed to land-use changes with afforestation.

1 | Introduction

The analysis of combined meteorological and streamflow data over a multi-century period provides progress in understanding the anthropic and climatic factors inducing changes in the hydrological cycle and supports the research in attribution science (Otto et al. 2016) and non-stationarity in geophysical processes (Montanari and Koutsoyiannis 2014; Singh et al. 2024). Compared to other climatological data such as precipitation or temperature, the availability of multi-century runoff data is, unfortunately, limited because of the complexity of the installation and maintenance of a hydrometric station, the geographical

This is an open access article under the terms of the Creative Commons Attribution License, which permits use, distribution and reproduction in any medium, provided the original work is properly cited.

© 2025 The Author(s). *Hydrological Processes* published by John Wiley & Sons Ltd.

and administrative fragmentation of river basins, and possibly because of weak coordination in sharing hydrometric data. For example, at the Global Runoff Data Center (GRDC 2021), daily runoff data longer than 160 years are available today for < 20 gauging stations worldwide and for just one station in the Mediterranean area, a very sensitive one to the impact of climate change (Noto et al. 2023) and, for this reason, worth investigating in detail.

Long-term hydrometric data collection and analyses are crucial for better control of the uncertainties in hydrologic design under uncertain future projections (Teegavarapu 2013). Substituting the length of time series by adding a large number of recent and short series, a common approach in regionalization studies (Hosking and Wallis 1997), does not meet the goal of studying the hydro-climatic features of the past and the comparison with present conditions in order to identify the causes of the non-stationarities. The weakness of 'trading space with time' becomes evident also for hydro-climatological and attribution studies in the current (Beniston et al. 1997) and projected climate (Gobiet et al. 2014) in mountain regions with gradients similar to the Alps, as Karakoram (Liaqat et al. 2022; Hasson et al. 2017) and Himalayas (Xiang et al. 2024). In the Sixth Assessment Report (IPCC 2022), the importance of trend analysis in runoff data is put in evidence when presenting the pattern of changes at the global level, also shown for the 1948–2004 period in Su et al. (2018). In the IPCC (2022, 662) report, runoff trends are analysed only for the 1971–2010 period, and they exhibit a very variable pattern also within continents, with increasing trends in Northern Europe, the Great Lakes region in North America, southern Brazil and Argentina, and decreasing trends in the Mediterranean basin, the East and West coasts in North America and central Brasil, respectively. Stahl et al. (2010), when analysing mean annual streamflow trends from 441 records of near-natural catchments in Europe in the period 1962–2004, found an exact balance of positive and negative trends but a systematic tendency of increasing trends in central and northern Europe and a decline in the Mediterranean and Danube area. Blöschl et al. (2017, 2019) found similar patterns by investigating spatial and temporal variability of floods in Europe over the 1960–2010 period. Focusing on the seasonality of flows, Zampieri et al. (2015), by analysing long-term discharge time series of the four major Alpine rivers, showed a tendency towards earlier spring peaks of more than 2 weeks per century, mainly due to the change in precipitation seasonality. Dealing with high-frequency fluctuations, Zolezzi et al. (2009), by processing streamflow time series for the Adige river from 1923 to 2006, highlighted an increase in small-scale fluctuations at the weekly scale in the last 50 years, due to the effect of reservoirs regulation for hydropower generation.

However, because analyses of multi-century daily streamflow are still scarce, any effort in analyzing long-term streamflow data within the scientific community is an added value to the debate on the changes in the hydrological cycle, drought and flood variability, especially when the link with climatic and anthropic changes is explored.

One objective of this study is the reconstruction and analysis of a complete long-term daily streamflow time series of the Adige river from the start of its water level recordings in 1862. A second objective is the identification of the likely natural climatic and anthropic drivers of the observed streamflow trends and variability at daily to multidecadal time scales in an intensively monitored mountain region, with marked orographic and climatic gradients (Rotach et al. 2009) and exploited for hydropower generation and irrigation, as in the Alps.

A third, more specific objective is to quantify the observed changes in the long term, at the annual, monthly, and daily scale, and to assess the magnitude of their likely causes. Both objectives are consistent with the urgent need of using high-quality observations for reducing uncertainties in predictions of the changes in the hydrological cycles induced by climatic and anthropic forcings (Ceola et al. 2016) and their impact on the availability of water resources for the needs of natural ecosystems and socio-economic activities (Schaefli et al. 2007; Gaudard et al. 2014).

In this paper, we describe, in the second section, the sources and the methods adopted to reconstruct the second longest time series of daily hydrometric levels and streamflow data for rivers, to the authors' knowledge, in the whole Mediterranean area. The time series obtained for the Adige river over the 1862–2022 period is analysed in the third section to identify changes in the monthly runoff regime in comparison with precipitation, temperature, and evapotranspiration, analysed in detail in a companion paper (Eccel and Ranzi 2025). There, a wavelet spectral analysis is conducted to highlight the effect of reservoirs on the daily streamflow in the last decades and to assess the coherence of runoff with climatic teleconnections as North Atlantic Oscillation (NAO), Western Mediterranean Oscillation (WeMO), and Atlantic Multidecadal Oscillation (AMO). In the fourth section, after comparing the results obtained for the Adige river basin with other European and Alpine rivers, we discuss the possible reasons for the observed increase in hydrological losses, decrease in runoff coefficient, and changes in spectral properties of the time series for the attribution to natural and anthropic causes. We propose future investigations to better address the uncertainties emerged in this study.

2 | Materials and Methods

2.1 | The Adige River Basin

Hydrological and meteorological observations were collected for the Adige river basin, in the Italian Alps, gauged at the Trento hydrometric station where the basin area measures 9763 km^2 (Provincia Autonoma di Trento 1978), including 130.5 km^2 in Switzerland, and altitude ranges from 186 m asl of the null point of the station to 3899 m asl of the Ortles peak (Figure 1). The mean altitude is 1735 m asl; glacierized areas decreased from 204 km^2 estimated in 1929 to 154 km^2 in the 1960s and to 100 km^2 in 2011 (Smiraglia and Diolaiuti 2015). The mainstream length is 156 km and land use is primarily woods (about 61%), meadows and pastures (20%), agricultural crops (4%), bare rocks (11%), and urban areas (2%) according to the 2018 CORINE land cover classification. Artificial reservoirs were constructed for hydropower generation starting in 1920 (Table 1 and Figure S1), and their total storage capacity

10991085, 2025, 11, Downloaded from https://onlinelibrary.wiley.com/doi/10.1002/hyp.70305 by Fondazione Edmund Mach, Wiley Online Library on [03/11/2025]. See the Terms and Conditions (https://onlinelibrary.wiley.com/terms-and-conditions) on Wiley Online Library for rules of use; OA articles are governed by the applicable Creative Commons License

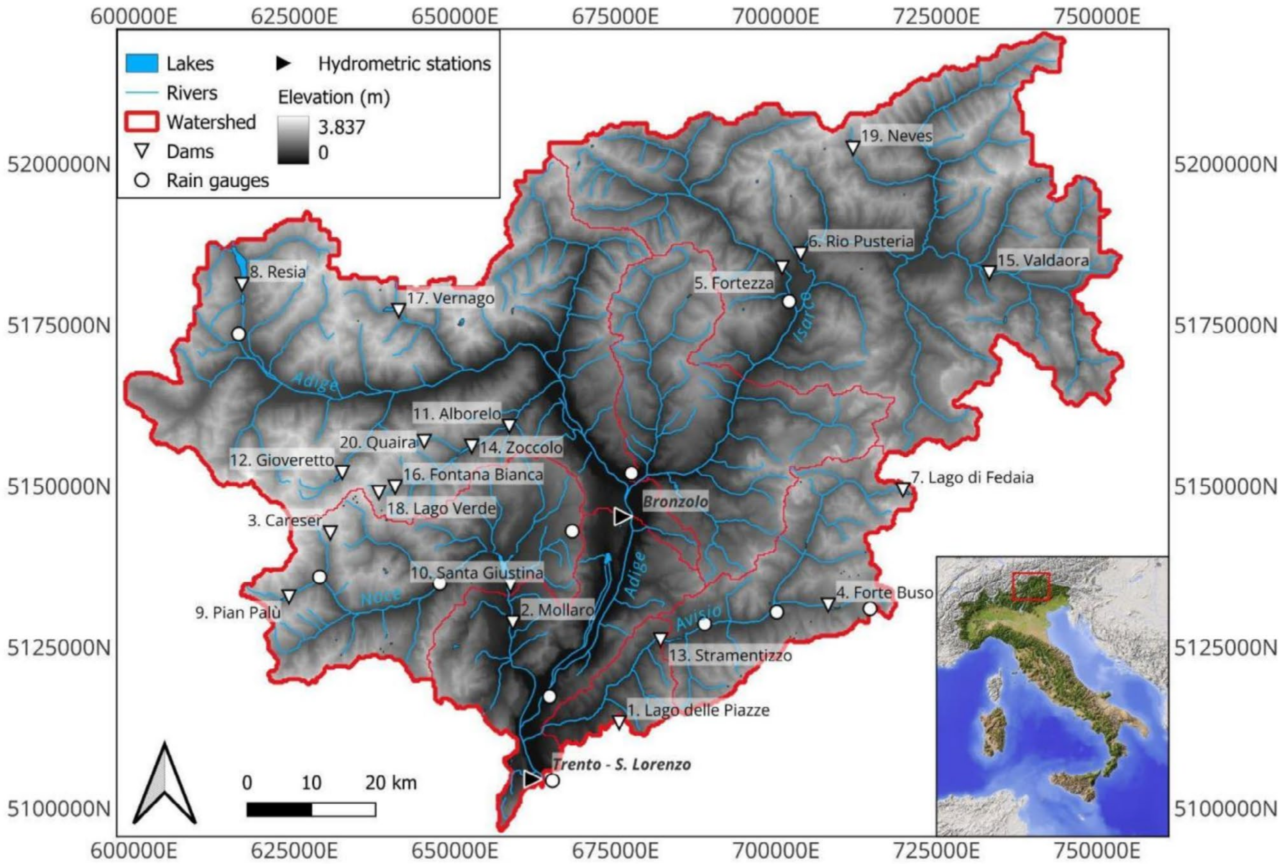

FIGURE 1 | The Adige river basin gauged at the Trento station (9793 km^2), raingauge stations used in this study and major reservoirs: their characteristics are reported in Table 1. Watershed divides of sub-basins used for the areal precipitation estimation are represented.

attained 552.36×10^6 m^3, corresponding to a specific volume of 56.6 mm and gauging a total basin surface of 5728.21 km^2, considering the area gauged by reservoirs located downstream in the respective rivers. The corresponding lake surface adds a surface of 19.27 km^2 to that ascribed to natural water bodies. Reservoirs with storage larger than 10×10^6 m^3 and suitable for annual regulation gauge an area of 2448 km^2, corresponding to about 25% of the total Adige catchment area. The reservoirs' volume does not take into account small reservoirs built in the latest decades for irrigation and artificial snowmaking. The volume stored in reservoirs constructed before 1945 accounts for only 10% of the total volume (Figure S1), and for this reason, in our work, the hydrometeorological regimes were analysed before and after this year. Two reservoirs constructed in 1939 and 1948 (nr. 4 and 7 in Figure 1 and Table 1), gauging a catchment area of 99.6 and 12.6 km^2, respectively, divert the streamflow, except the environmental flow and the excess discharge from the spillways during major floods, from the Avisio, left-side tributary of the Adige river, to other basins, and this effect was accounted for in computing the specific runoff volumes by subtracting the area gauged by the two reservoirs. The objective of all the reservoirs with major storage capacity, as reported in Figure 1 and Table 1, is hydropower generation. Only recently, following the enforcement of the 2007/60/EC Water Flood Directive and the Flood Management Plans, the reservoirs have been used also for flood control, especially during the autumn flood season. Rules are set in the Flood Management Plans (Provincia Autonoma di Trento 2015).

2.2 | Hydrometric Data Collection and Reconstruction

In this study, to better analyse the joint long-term variability of meteorological and hydrological regimes, a specific effort was made to extend the hydrometric series of the Adige river in Trento as far back in the past as possible. For this purpose, we digitised the records with the manual readings of the water level at S. Lorenzo bridge hydrometric station in Trento (TSL in the following) in the town Municipal Historical Archives (Albertelli 2014). These data, not published yet, to the knowledge of the authors, include readings conducted by officers of the Trento Municipality every 2 days starting on 2nd January 1862 until 31st December 1865 and then daily readings until 31st December 1927. The official hydrometric null point was set to 186.09 m asl. Official daily water level data recorded generally at 7 am by an independent observer and published by the Austrian Hydrographic Service in the Hydrological Yearbooks from 1st January 1893 to 31st December 1912 were also available for verification (all the region was part of the Austro-Hungarian Empire until 1918). The mean difference between the two records is just 0.2 mm, and the mean absolute error between the two readings is 36 mm, thus supporting the reliability of the two independent sources of information. Readings conducted every 2 days in the years 1862 until 1865 were linearly interpolated to obtain daily values, and for the period common to the two series, the data of the Trento Municipality were adopted, for the sake of homogeneity of the source and after having noted some evident typing errors in the Hydrological Yearbooks. Hydrometric readings

10991085, 2025, 11, Downloaded from https://onlinelibrary.wiley.com/doi/10.1002/hyp.70305 by Fondazione Edmund Mach, Wiley Online Library on [03/11/2025]. See the Terms and Conditions (https://onlinelibrary.wiley.com/terms-and-conditions) on Wiley Online Library for rules of use; OA articles are governed by the applicable Creative Commons License

TABLE 1 | Characteristics of the reservoirs with storage capacity greater than $0.5 \times 10^6\,m^3$ in the Adige river basin (PAT 1978).

Reservoir name	Year of impoundment	Storage capacity ($10^6\,m^3$)	Lake's surface (km^2)	Surface of the gauged basin (km^2)
1. Piazze	1920	6.70	0.37	*35.00*
2. Mollaro	1928	0.88	0.16	*1225.00*
3. Careser	1931	17.00	0.47	10.40
4. Forte Buso	1939	32.00	0.69	99.55
5. *Fortezza*	1940	3.30	0.23	*680.00*
6. Rio Pusteria	1940	2.04	0.26	*1940.00*
7. Fedaia	1948	17.23	0.55	12.59
8. Resia	1949	118.10	6.60	*310.00*
9. Pian Palù	1951	15.90	0.57	35.20
10. S. Giustina	1951	182.81	3.46	1050.00
11. Alborelo	1953	3.30	0.17	214.00
12. Gioveretto	1955	19.90	0.70	*103.00*
13. Stramentizzo	1956	13.60	0.65	*617.91*
14. Zoccolo	1957	33.50	1.43	*181.20*
15. Valdaora	1959	6.10	0.44	594.00
16. Fontana Bianca	1959	1.48	0.15	66.75
17. Vernago	1963	42.20	1.00	*150.10*
18. Lago Verde	1963	7.20	0.24	13.50
19. Neves	1965	15.10	0.48	36.60
20. Quaira	1967	12.80	0.35	75.00
Others	—	1.22	0.30	811.5 (*486.00*)
Total	—	552.23	19.27	*5728.21*

Note: In italic the area gauged by reservoirs located more downstream in the respective rivers.

until 24 April 1864, were corrected for the 0.316 m downward shift of the null point of the hydrometric station as documented by von Weber Ebenhof (1892, 227). A recording gauge was installed in June 1921. After 16th February 1919, daily water level and after 1st January 1923, the mean daily streamflow were measured and processed first by the Water Magistrate of Venice until 1974, then, from 1975 until 1988, by the Trento Province Hydrographic Service and finally, until 31st December 2022, by the Office of Hydraulic Works of the Autonomous Province of Trento. Water level data at TSL, h_{TSL} (water depth above the null point in meters), are complete, but, as pointed out by Zolezzi et al. (2009), who analysed the Trento hydrometric series from 1923 until 2008, the official time series of daily streamflow data shows a gap between 1944 and 1950 because of the damages to the steel bridge without piers downstream the cross section during WWII. As in the above-mentioned paper, for the year 1944, we adopted the data reconstructed through a linear regression between TSL and the measured streamflow at a second gauging station far downstream, Boara Pisani. To fill the gap of discharge data for the years 1945–1948, we also used streamflow data recorded at Serravalle gauging station, 35 km downstream of Trento. For the year 1949, when the new bridge with a new structure and two piers was completed, and 1950, we reconstructed the streamflow data, Q_{TSL} ($m^3\,s^{-1}$) with the stage-discharge curve based on the discharge measurements conducted in the year 1951 at the TSL hydrometric station:

$$Q_{TSL} = 79.356\,h_{TSL}^2 + 2.174 h_{TSL} + 54.311 \quad (1)$$

For the period between 1944 and 1950, the uncertainty of streamflow reconstruction does not meet the standards in hydrometry (WMO 2010), however, the cross section was regular and the overall uncertainty of daily discharge measurements can be assessed at about 10%. For the remaining period between 1923 and 2022, standard measurements with current meters and the velocity-area method were conducted and the daily discharge uncertainty can be assessed to be about 5%.

More complex was the reconstruction of daily streamflow based on the daily water level observations conducted from

10991085, 2025, 11, Downloaded from https://onlinelibrary.wiley.com/doi/10.1002/hyp.70305 by Fondazione Edmund Mach, Wiley Online Library on [03/11/2025]. See the Terms and Conditions (https://onlinelibrary.wiley.com/terms-and-conditions) on Wiley Online Library for rules of use; OA articles are governed by the applicable Creative Commons License

January 1862 to December 1922. In this period, the available sources were: (i) 10 diagrams of surface velocity profiles conducted by Annibale Apollonio, director of the technical office of Trento Municipality, in the years 1882–1889 (von Weber Ebenhof 1892), (ii) four more measurements of maximum surface velocity conducted from 1882 until 1884 (Figure 2a), (iii) one discharge estimate for the September 1882 flood based on these measurements (Apollonio 1885; Municipio di Trento 1889), and (iv) eight standard discharge measurements conducted between 1901 and 1907 with a Woltman current meter and the velocity-area method (Hydrographischer Dienst Österreich, years 1901–1907 in Kommission bei W. Braumüller 1903). From the complete measurements conducted in the 1901–1907 period, it was possible to estimate the entropic parameter, M, of the model which links maximum surface velocity, $V_{\max}$, and mean velocity, V_m, in the river cross section after the simplification introduced by Moramarco et al. (2004) of the Chiu (1988) model based on the entropic hydrodynamic theory applied to open channel flow,

$$V_m = \Phi(M)\, V_{\max} = \left(\frac{e^M}{e^M - 1} - \frac{1}{M} \right) V_{\max} \tag{2}$$

with the 0.753 value obtained for $\Phi(M)$, and M resulting equal to 3.3, from a best fit from the eight discharge measurements in the 1901–1907 period, the nine surface velocity profiles measured in the 1882–1884 period were useful to estimate the mean velocity and, given the river cross-section, the discharge. These data were adopted to calibrate the roughness coefficient in the Chezy stage-discharge equation adopted for the 1862–1922 period. It is worth noticing that one additional surface velocity profile measured during the flood of 12 October 1889, after the recalibration of the cross section conducted in that year, and a stage of 5.20 m over the null point, exhibited the same maximum velocity of 4.36 $\mathrm{m\,s^{-1}}$ measured with the same water level during the flood of 19 September 1882, thus confirming that the hydrodynamics of the river cross section remained stable throughout the 1882–1907 period. Figure 2a shows, as an example, the stage-discharge curve adopted for the 1882–1889 period. The overall verification of the discharge measurements vs. stage-discharge estimates for the period 1862–1922 is shown in Figure 2b and can be considered very satisfactory for the medium-to-high flow range. The geometry of the cross section was derived from the drawings of the Adige river regulation projects, the Dorigo (1967) technical report, the notes about changes occurred between the 1860s and the 1890s in the thalweg bottom reported in von Weber Ebenhof (1892) and the trends of the minimum water levels observed in that period, as visible also in Figure 3 as the lower envelope of the water levels. For the hydraulic head slope J in the Chezy equation we adopted the average value $J = 0.001116$, observed in the discharge measurements conducted in the 1901–1907 period. The Gauckler-Strickler roughness coefficient resulting from the best fit of discharge estimated after the nine measurements of surface velocity profiles in the 1882–1884 period was $K_s = 31\,\mathrm{m^{1/3}\,s^{-1}}$ and was adopted for the period 1862–1894. After the works of recalibration of the cross section completed in 1895, with the construction of a new steel bridge without piers, because the comparison of photographs put in evidence a smoothing of the surface of the river banks, a value of $K_s = 33\,\mathrm{m^{1/3}\,s^{-1}}$ was estimated, consistent with the runoff measurements conducted between 1901 and 1929. This value was adopted for the reconstruction of the stage-discharge curve in the 1895–1922 period, before the official streamflow measurements started to be published routinely in the hydrological yearbooks. A verification of the stage-discharge curve reconstructed for this period without official streamflow measurements was conducted with the first official discharge measurements of the Italian Hydrographic Service and is given in Figure 2c; the discharge curves estimated for the 1917–1921 period, considering also the changes in the cross section with the slow rise of the thalweg after the 1890s hydraulic works, were compared with the flow measurements conducted with the velocity-area method in the 1923–1928 period. Also, in this case the comparison is satisfactory, confirming the reliability of the method adopted.

2.3 | Meteorological Data: Sources and Pre-Processing

The archive sources for precipitation and temperature monthly series were different:

- homogenised series from the HISTALP database on Alpine meteorological stations (Auer et al. 2007);
- original series from the Meteorological Services of Trento and Bolzano provinces and from Fondazione E. Mach;
- one series (Cavalese) of daily precipitation, partially transcribed from the original daily paper records collected at the local monastery of Franciscan monks (Brugnara and Maugeri 2019; Colombo 2016; Scolozzi and Eccel 2017).

Precipitation series underwent two quality-improving processes: (i) rain gauge loss rates of the snow fraction of the precipitation, responsible for a systematic underestimation (Grossi et al. 2017); (ii) adjustment for the elevation-dependent amount increase due to orographic effects on the precipitation rates. A general anagraphic table of all stations can be found in Eccel and Ranzi (2025), where details on the creation and homogenization of the series can be found in the Supporting Information file. All series were gap-filled and checked for their homogeneity.

2.4 | Water Balance

The balance quantities were calculated by function "thornthwaite" in R package "ClimClass" (Eccel et al. 2015), freely available at the R platform (R Core Team 2025). The water balance algorithm is adapted from Thornthwaite and Mather (1955, 1957), including a temperature threshold for snow precipitation, monthly fractions of snow melt computed with a melt factor, soil field capacity for soil moisture accounting, and estimation of the water desiccation law. It runs on monthly series of temperature and precipitation, driven by the following processes:

- snow accumulation and melting;
- water infiltration and soil storage;
- evapotranspiration;
- runoff.

10991085, 2025, 11, Downloaded from https://onlinelibrary.wiley.com/doi/10.1002/hyp.70305 by Fondazione Edmund Mach, Wiley Online Library on [03/11/2025]. See the Terms and Conditions (https://onlinelibrary.wiley.com/terms-and-conditions) on Wiley Online Library for rules of use; OA articles are governed by the applicable Creative Commons License

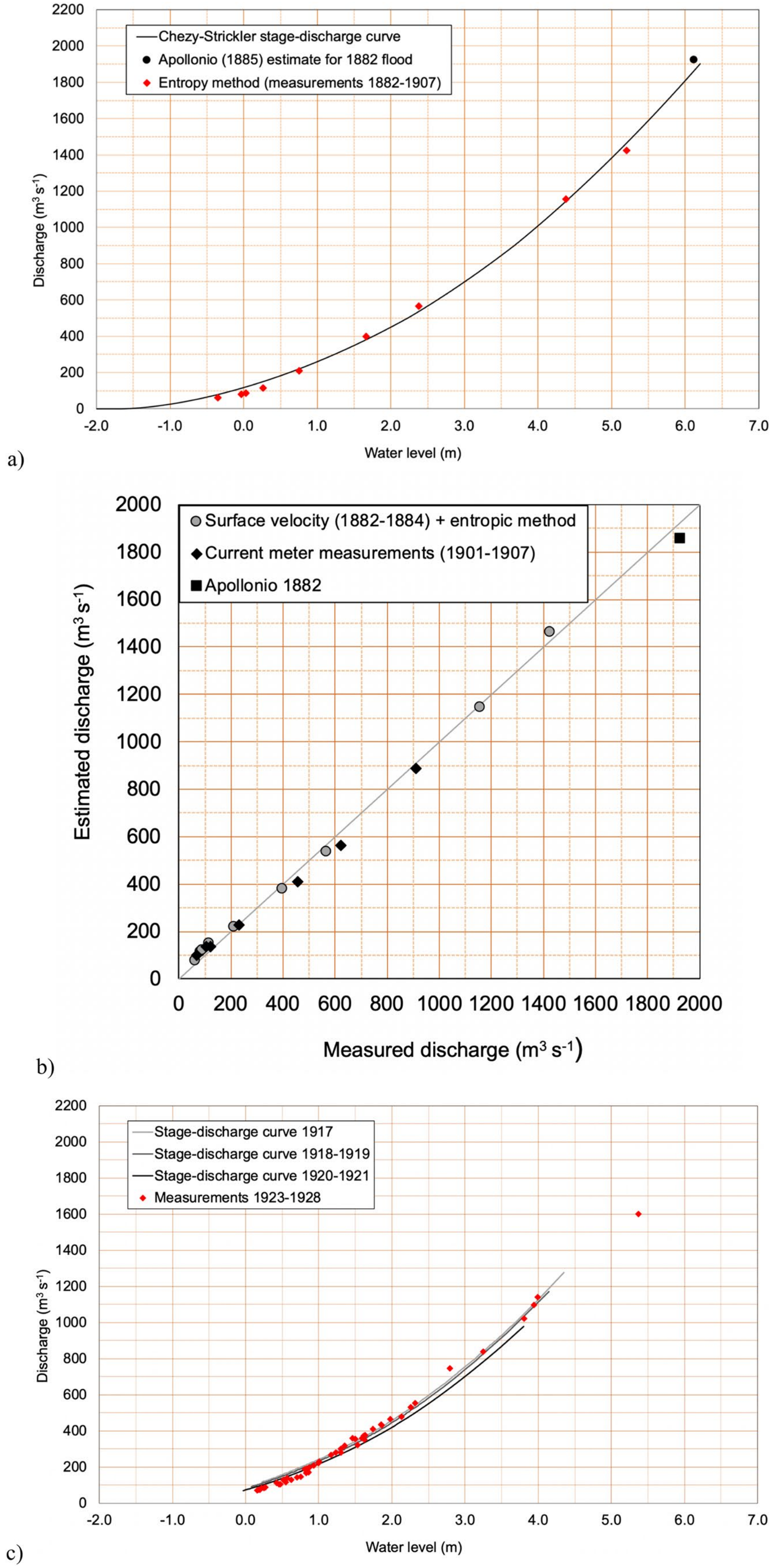

FIGURE 2 | Stage-discharge curve (a) calibrated for the Adige in Trento hydrometric station in the period 1882–1884 and based on the surface velocity and discharge measurements in the period 1882–1907; (b) verification of the discharge estimation over the 1882–1907 period; (c) ex-post verification of the estimated stage-discharge curve in the 1917–1921 period with the first measurements of the Italian Hydrographic Service in the 1923–1928 years.

10991085, 2025, 11, Downloaded from https://onlinelibrary.wiley.com/doi/10.1002/hyp.70305 by Fondazione Edmund Mach, Wiley Online Library on [03/11/2025]. See the Terms and Conditions (https://onlinelibrary.wiley.com/terms-and-conditions) on Wiley Online Library for rules of use; OA articles are governed by the applicable Creative Commons License

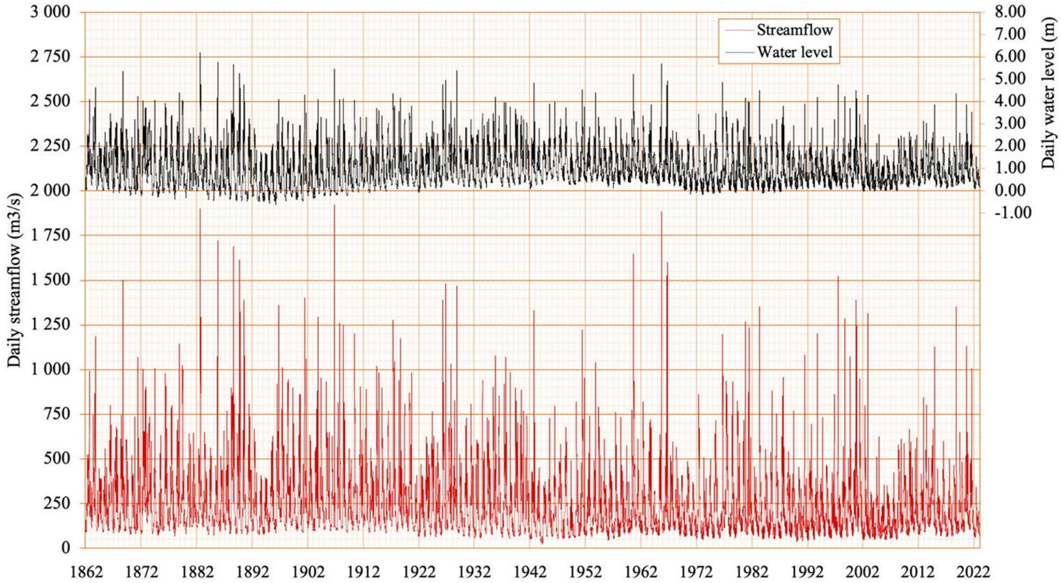

FIGURE 3 | Time series (1862–2022) of the daily water level measurements and daily streamflow estimates for the Adige river in Trento.

Potential evapotranspiration is calculated as a non-linear function of mean monthly temperature, modulated by an "annual thermal index" and referred to as the relative daylength. Actual evapotranspiration equals potential evapotranspiration when there is no limitation in soil water availability; on the contrary, the evapotranspiration rate is diminished according to soil deficit, calculated via a water desiccation law, which is in turn a function of potential evapotranspiration. The Thornthwaite algorithm was applied to all the monthly series at each grid point. Finally, the output (monthly series of all water balance variables) for the grid points was averaged to get unique, basin-representative series (see more details on the spatial data processing in the next section). The model skill for the Adige river basin was tested by a comparison of results with simulations for the nearby Adda river, giving very positive results. For more details on the algorithm and model validation, please see Eccel and Ranzi (2025).

These series, like the monthly series of precipitation and mean temperature, were aggregated to produce annual series for both annual and seasonal (DJF for winter and so on) aggregations.

2.5 | Teleconnections

The hydrological regimes of large rivers can be determined by the prevailing meteorological conditions during a period (months to years), in turn driven by large-scale atmospheric circulation patterns; among these, particularly important is the North Atlantic Oscillation (NAO), whose role has been ascertained as the main factor explaining anomalies in winter precipitation and temperature in Europe and in the Mediterranean (Trigo et al. 2002; Hurrell et al. 2003). In the Alpine region, the relationship between water balance anomalies and the atmospheric precursor NAO is more complex, being the region in the transition zone between the European northern area—experiencing warm and wet conditions during positive phases—and the southern one, experiencing drier conditions, and only small temperature deviations from the normal (Wanner et al. 2001; Marzeion and Nesje 2012). However, being this pattern the most important player in seasonal variability of hydrological regimes, the use of a quantitative index of NAO (NAOI) has been considered also for runoff prediction purposes (Bierkens and van Beek 2009; Steirou et al. 2017). Ranzi et al. (2024) found a negative correlation, ranging between −0.37 and −0.52, between NAOI and the snow water equivalent (SWE) accumulated in the western Adige river basin on the 1st and on the 15th of April and a weaker positive correlation with the Western Mediterranean Oscillation (WeMO). Brugnara and Maugeri (2019) indicate a relevant influence of the Atlantic Multidecadal Oscillation (AMO) on the daily precipitation regime in the southern Alps. Therefore, we analyzed the coherence of indices of AMO, NAO, and WeMO with the monthly streamflow and precipitation data to obtain the wavelet coherence spectra.

2.6 | Statistical and Spectral Analyses

Statistical and spectral analyses were conducted for the time series of precipitation, streamflow, runoff coefficient, and hydrological losses. Theil-Sen slopes were estimated on the entire time series and in sub-periods before and after 1945, when the constructions of reservoirs accelerated, as shown in Table 1 and Figure S1. The null hypothesis of non-existence of a monotonic trend in the series was tested with the Mann-Kendal test with a 5% significance level.

A second analysis was performed in order to identify transients of persistent dry or wet periods in the time series of annual precipitation and runoff volumes. It consists of a Moving Average and Running Trend Analysis, adopted in Ranzi et al. (2024) in analyzing SWE statistics in the Alps, similarly to that reported in Brunetti et al. (2009). MARTA consists of computing the centered moving average and the running trend slope for all the possible sub-periods longer than a threshold value (20 years in our case), reporting the results in a chart where the central year of the sub-period is reported on the horizontal axis and its length on the vertical one.

10991085, 2025, 11, Downloaded from https://onlinelibrary.wiley.com/doi/10.1002/hyp.70305 by Fondazione Edmund Mach, Wiley Online Library on [03/11/2025]. See the Terms and Conditions (https://onlinelibrary.wiley.com/terms-and-conditions) on Wiley Online Library for rules of use; OA articles are governed by the applicable Creative Commons License

In addition to MARTA triangles, a second spectral analysis was conducted using wavelets, very effective in localising signal energy at different temporal scales in the time domain. The streamflow series was first normalised by subtracting the long-term mean and dividing by the standard deviation, so that the annual cycle was not removed; then the wavelet transform with the Morlet-6 basis function was conducted using a package developed by Torrence and Compo (1998). Wavelets were also used to obtain the wavelet coherence spectra between streamflow and the above-mentioned teleconnection indices.

3 | Results

3.1 | The Reconstructed Hydrometric Time Series (1862–2022)

The resulting time series of daily water level and daily discharge is shown in Figure 3 and with its 161-year duration, it represents the second longest hydrometric series of daily discharge for Italian rivers after the 172-year-long series of the Adda river (Ranzi et al. 2017, 2021) made available also at the Global Runoff Data Center (GRDC 2021).

Because uncertainties arise from the reconstruction of daily runoff in the period prior to 1923, when systematic official discharge measurements started, for verification purposes, the cumulative runoff volumes were compared with those of the nearby Adda and Oglio rivers, for which a high-quality streamflow time series was available. The agreement is satisfactory (see further in Section 4) and does not show systematic biases, thus supporting the validity of the analyses conducted and the reconstructed time series. By applying international ISO standards for discharge measurements uncertainty assessment (WMO 2010) and with reasonable assumptions on the cross section and roughness uncertainties, as in Di Baldassarre and Montanari (2009), Albertelli (2014) estimated a 10% standard uncertainty with a 95% confidence level for annual streamflow prior to 1923, and a 5% standard uncertainty in the following period, with the exception of the period 1944–1950, when the discharge was estimated from hydrometric measurements downstream, as already stated, and was more uncertain.

3.2 | Changes in Annual Precipitation and Runoff Trends

Reconstructed streamflow time series enable several analyses, starting with the trend analysis of the mean annual flow and runoff coefficient. For this purpose, the specific streamflow volume was computed and compared with both mean precipitation and the runoff coefficient that is, the ratio of the two, calculated according to the hydrological year, starting in September of the previous year, after the summer maximum precipitation period, and before the beginning of the autumn and winter snowfall. The analysis was conducted for two periods: the first one covers the 150 years 1862–2011 ('climatological 150-year period' from now on), encompassing five 30-year spans, a standard length adopted for climatology analyses, and focusing on precipitation, temperature, and actual evapotranspiration. The figures show that annual precipitation (949 mm on average for the 'climatological period') exhibits a slight decrease, with a −0.19 mm year^{-1} Theil-Sen slope of the regression line over time, a value non-significantly different from zero, while the mean annual streamflow (716 mm on average) and the runoff coefficient (0.75 on average) are significantly declining with a −1.2 mm year^{-1} Theil-Sen slope of the regression line for runoff. The trend is confirmed when analysing the entire monitoring period 1862–2022 as shown in Table 2 and in Figure 4. A Mann-Kendall test with a 5% significance level confirms the results from the visual inspection, with a statistically non-significant decrease of precipitation (with a 951 mm average, a slope of −0.19 mm year^{-1} and a Mann-Kendall $Z = -0.69$) and a significant decrease of runoff, instead (with a 713 mm average and a Mann-Kendall $Z = -4.91$). The observed −1.0 mm year^{-1} slope of the annual runoff trend indicates a decline of −1.2% per decade from the start of the time series, similar to the ones observed in nearby basins (Ranzi et al. 2017, 2021). As a consequence of the different trends of precipitation and runoff, the runoff coefficient, computed for the hydrological years, decreases with a 5% statistical significance at a rate of −0.010 decade^{-1} (Figure 4 and Table 2).

3.3 | Variability at Different Temporal Scales: MARTA Triangles

In the chart of the running trends, computed by least-square linear regression, slopes are represented by the pixel colour. Their size is an index of the significance level of a statistical test for the existence of trends, being thicker where a 5% significance level of the Mann-Kendall test is assessed (Figure 5). The figure is completed, when appropriate, with a vertical change-point line when the null hypothesis H_0 of no change is rejected applying, with a 5% significance level, the Pettitt test, a non-parametric technique to solve the change-point problem (i.e., identifying if and when the probability distribution of a stochastic variable has changed). In addition, the MARTA triangles in Figure 5 indicate no significant trends of precipitation throughout the climatological observation period, while runoff declines significantly for all time windows longer than 80 years. At shorter time scales, transients of significantly drier periods around the 1940s, when a severe drought occurred in northern Italy, become evident both in precipitation and runoff, as well as wetter periods in the 1960s and 1970s, as emerged also in the analysis of accumulated SWE in the Italian Alps including the Adige river basin (Ranzi et al. 2024). The change-point line on the runoff chart just before the 1940s dry period and its absence in the precipitation chart shows not only the discontinuity of the 1940s drought but also a more significant decline in runoff than in precipitation.

3.4 | Changes in Monthly Precipitation and Runoff Regimes

The distribution of monthly precipitation in the year changed slightly over the monitoring period. Statistics were estimated before and after 1945, when the construction of reservoirs accelerated, and because a change point in the runoff regime was identified in the 1940s, as recalled in the previous section. The

10991085, 2025, 11, Downloaded from https://onlinelibrary.wiley.com/doi/10.1002/hyp.70305 by Fondazione Edmund Mach, Wiley Online Library on [03/11/2025]. See the Terms and Conditions (https://onlinelibrary.wiley.com/terms-and-conditions) on Wiley Online Library for rules of use; OA articles are governed by the applicable Creative Commons License

TABLE 2 | Statistics of the time series of annual values of hydrometeorological variables in the solar years.

	Precipitation P (mm)	Runoff Q (mm)	Runoff coefficient (–)	Hydrological losses $L = P - Q$ (mm)
Mean (1862–2022)	951	713	0.75	239
Slope (mm year^{-1})	−0.19 [−0.75, 0.34]	**−1.01 [−1.46, −0.61]**	**−0.010 decade^{-1} [−0.013, −0.008]**	**0.86 [0.55, 1.13]**
Change rate (% decade^{-1})	−0.2	**−1.4**	**−1.2**	**4.9**
Mean (1862–2011)	949	716	0.75	233
Mean (1862–1945)	964	759	0.79	205
Mean (1946–2011)	930	662	0.71	268
Mean (1946–2022)	937	664	0.71	273

Note: Statistics for the runoff coefficient and the hydrological losses are presented for the hydrological years (September–August). Mean values are presented for the entire monitoring period (1862–2022) and for the 'climatological 150-year period' (1862–2011). Mean annual values are computed also for the periods before and after 1945 when the construction of reservoirs accelerated. Trend slopes, with 95% confidence intervals in square brackets, are marked in bold when the null hypothesis of no trend in the Mann-Kendall test is rejected with a 5% significance level.

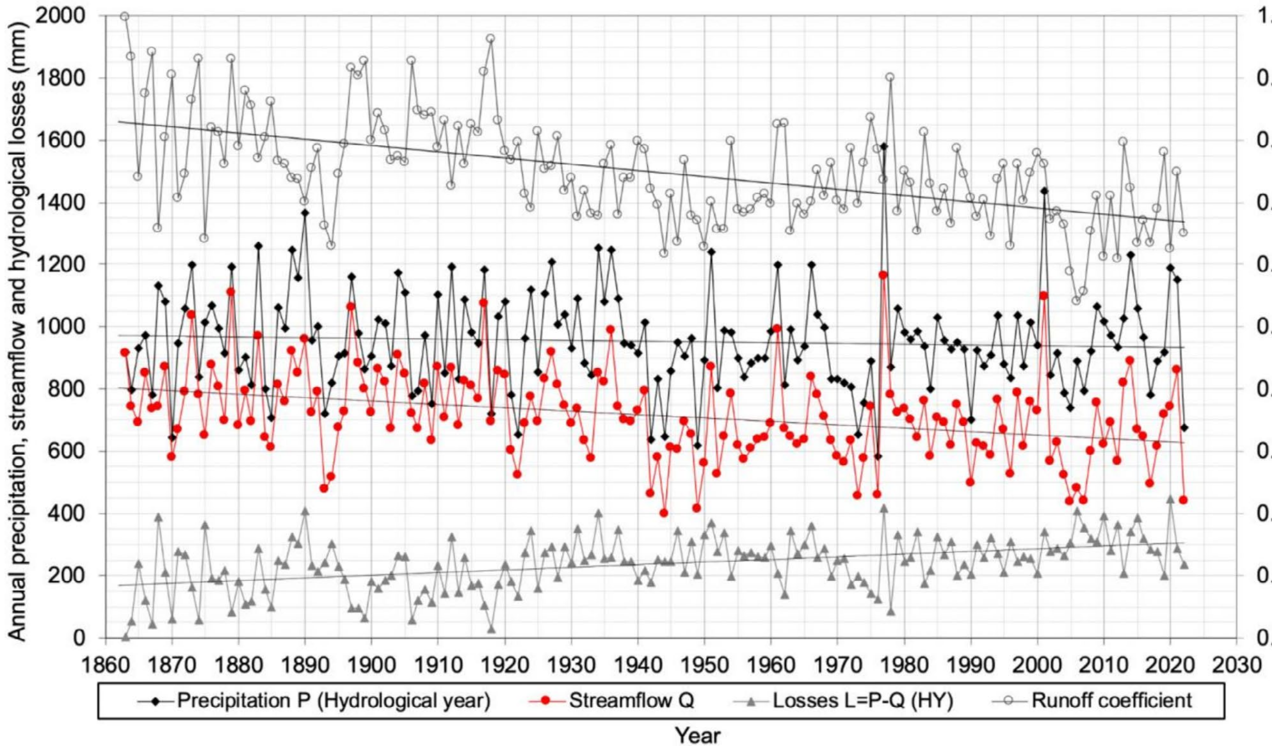

FIGURE 4 | Annual precipitation, streamflow, hydrological losses, and runoff coefficient of the Adige river basin in the hydrological years starting with September 1862 until August 2022.

slight decline of annual precipitation is evidenced in Table 2, with a decrease from 964 mm before 1945 to 937 mm after that year until 2022. Streamflow volumes decreased more significantly from 759 to 664 mm, as did the runoff coefficient, from 0.79 to 0.71. The monthly distribution of precipitation exhibits a decrease in March, September, and October and an increase in August and November in the recent decades (Figure 6, and comparison of Tables 3 and 4) and is consistent with a recent climatology for the region reported in Crespi, Matiu, et al. (2021). In Table S1, statistics for solar years in the pre-reservoirs period are reported for a comparison with values in Tables 3 and 4. A similar shift, except the increase in August, was also observed for the Adda river basin in the 1845–2016 period investigated in Crespi, Brunetti, et al. (2021) and in Ranzi et al. (2021).

Monthly runoff distribution changed differently than precipitation: an increase in winter plus March (DJFM) is compensated by a decrease in summer (JJA) (Figure 7, S3, S4, S5 and comparison of Table 3 and Table 4). The increase of runoff in the winter period during the completion of reservoirs (1946–2022) at a rate of +0.345 mm year^{-1}, is statistically significant, as shown in Table S3. The decrease in summer runoff (JJA) after 1945 is statistically significant, at a rate of −0.647 mm year^{-1} (Figures S6, S7 and Table S3).

10991085, 2025, 11, Downloaded from https://onlinelibrary.wiley.com/doi/10.1002/hyp.70305 by Fondazione Edmund Mach, Wiley Online Library on [03/11/2025]. See the Terms and Conditions (https://onlinelibrary.wiley.com/terms-and-conditions) on Wiley Online Library for rules of use; OA articles are governed by the applicable Creative Commons License

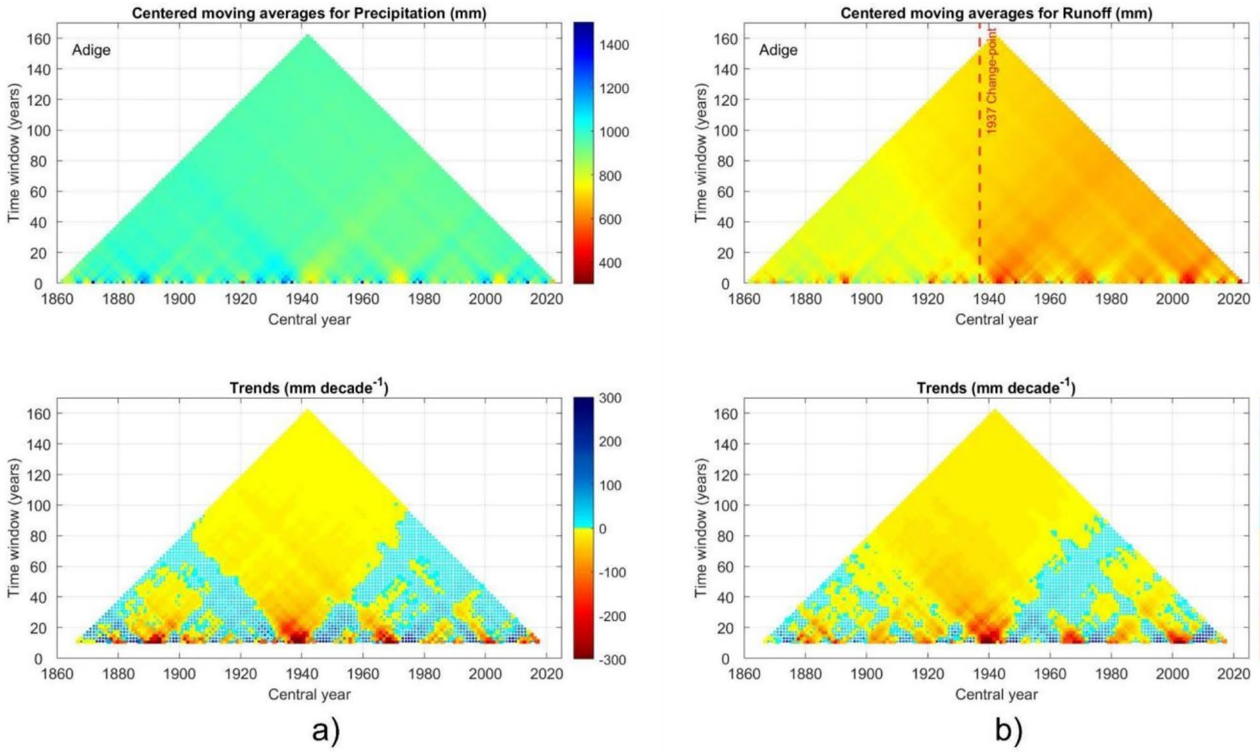

FIGURE 5 | Moving Average Running Trend Analysis (MARTA) triangles with centred moving averages (top panels) and Sen-Theil trend slopes (bottom panels) of (a) precipitation (left) and (b) runoff (right) at different scales. In the top right panel the year of the change point estimated with the Pettitt test is marked with a red dashed line. In the bottom graphs the trends with 5% significance level of the Mann–Kendall test are reported as thicker pixels.

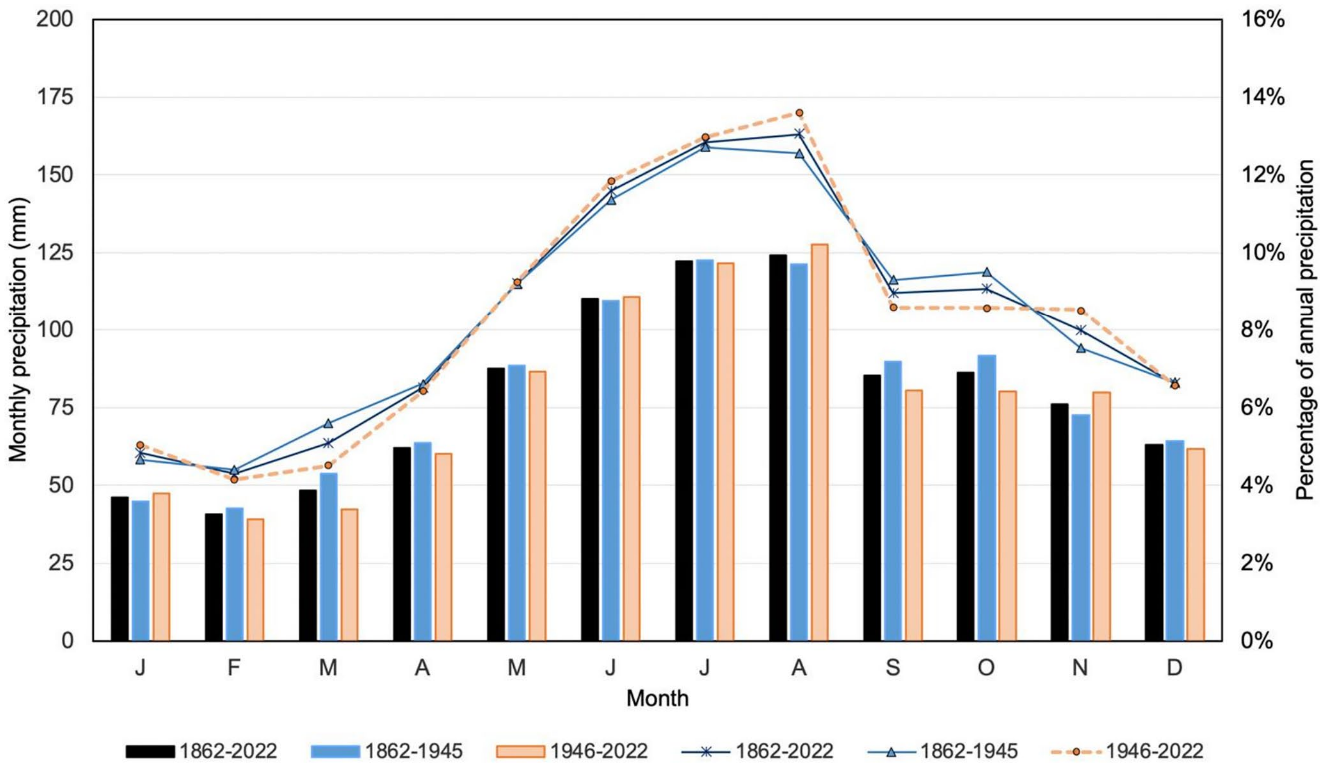

FIGURE 6 | Monthly precipitation regime and percentage of mean annual precipitation in the Adige river basin for the monitoring periods 1862–2022, before (1862–1945) and after (1946–2022) the construction of major reservoirs.

10991085, 2025, 11, Downloaded from https://onlinelibrary.wiley.com/doi/10.1002/hyp.70305 by Fondazione Edmund Mach, Wiley Online Library on [03/11/2025]. See the Terms and Conditions (https://onlinelibrary.wiley.com/terms-and-conditions) on Wiley Online Library for rules of use; OA articles are governed by the applicable Creative Commons License

TABLE 3 | Monthly hydrological regime and the solar year annual precipitation, runoff, and runoff coefficient for the Adige river basin in the period 1862–2022.

Month	Precipitation (mm)	Streamflow ($m^3 s^{-1}$)	Runoff (mm)	Runoff coefficient (–)
J	46.0	111.2	30.7	0.67
F	*40.8*	*106.1*	*26.7*	*0.65*
M	48.3	121.9	33.7	0.70
A	62.0	170.3	45.5	0.73
M	87.6	313.4	86.5	**0.99**
J	110.1	**409.2**	**109.2**	**0.99**
J	122.1	341.4	94.2	0.77
A	**124.1**	276.1	76.2	0.61
S	85.2	236.2	63.1	0.74
O	86.2	215.6	59.5	0.69
N	76.0	190.9	51.0	0.67
D	62.9	134.2	37.0	0.59
Year	951.3	220.6	713.2	0.75

Note: Monthly maxima in bold and minima in italics. When computing the specific runoff (in mm), the area gauged by reservoirs with diversion outside the catchment was considered, and the streamflow in $m^3 s^{-1}$ was computed accordingly.

TABLE 4 | Monthly hydrological regime and the solar year annual precipitation, runoff, and runoff coefficient for the Adige river basin in the period 1946–2022, when the influence of reservoirs was more relevant.

Month	Precipitation (mm)	Streamflow ($m^3 s^{-1}$)	Runoff (mm)	Runoff coefficient (–)
J	47.2	112.4	31.2	0.66
F	*38.9*	110.6	*28.0*	0.72
M	42.2	122.3	34.0	0.80
A	60.2	161.3	43.4	0.72
M	86.5	288.4	80.1	**0.93**
J	110.8	**367.2**	**98.7**	0.89
J	121.5	303.3	84.2	0.69
A	**127.5**	245.3	68.1	*0.53*
S	80.4	213.4	57.4	0.71
O	80.3	195.5	54.3	0.68
N	79.8	181.3	48.7	0.61
D	61.6	128.1	35.6	0.58
Year	936.8	205.3	663.6	0.71

Note: Monthly maxima in bold and minima in italics. When computing the specific runoff (in mm), the area gauged by reservoirs with diversion outside the catchment was considered, and the streamflow in $m^3 s^{-1}$ was computed accordingly.

3.5 | Wavelet Spectrum of Streamflow and Coherence With Climatic Teleconnections

Figure 8 shows the result of this analysis, whereas the spectrum we obtained for both normalized and deseasonalized records of daily flows is reported in Figure S2. High energy with a 5% significance level, indicated by the black contour lines, remains at a 3-month period and around 11 years, as also found for the Adda river in Ranzi et al. (2021) and, in the last decades, also at the weekly time scale. The energy signal appears to be stationary in the early period, when 'natural' conditions prevailed. After 1945, instead, energy on a weekly scale increases steadily until the end of the century, to decline later (Figure 9a).

10991085, 2025, 11, Downloaded from https://onlinelibrary.wiley.com/doi/10.1002/hyp.70305 by Fondazione Edmund Mach, Wiley Online Library on [03/11/2025]. See the Terms and Conditions (https://onlinelibrary.wiley.com/terms-and-conditions) on Wiley Online Library for rules of use; OA articles are governed by the applicable Creative Commons License

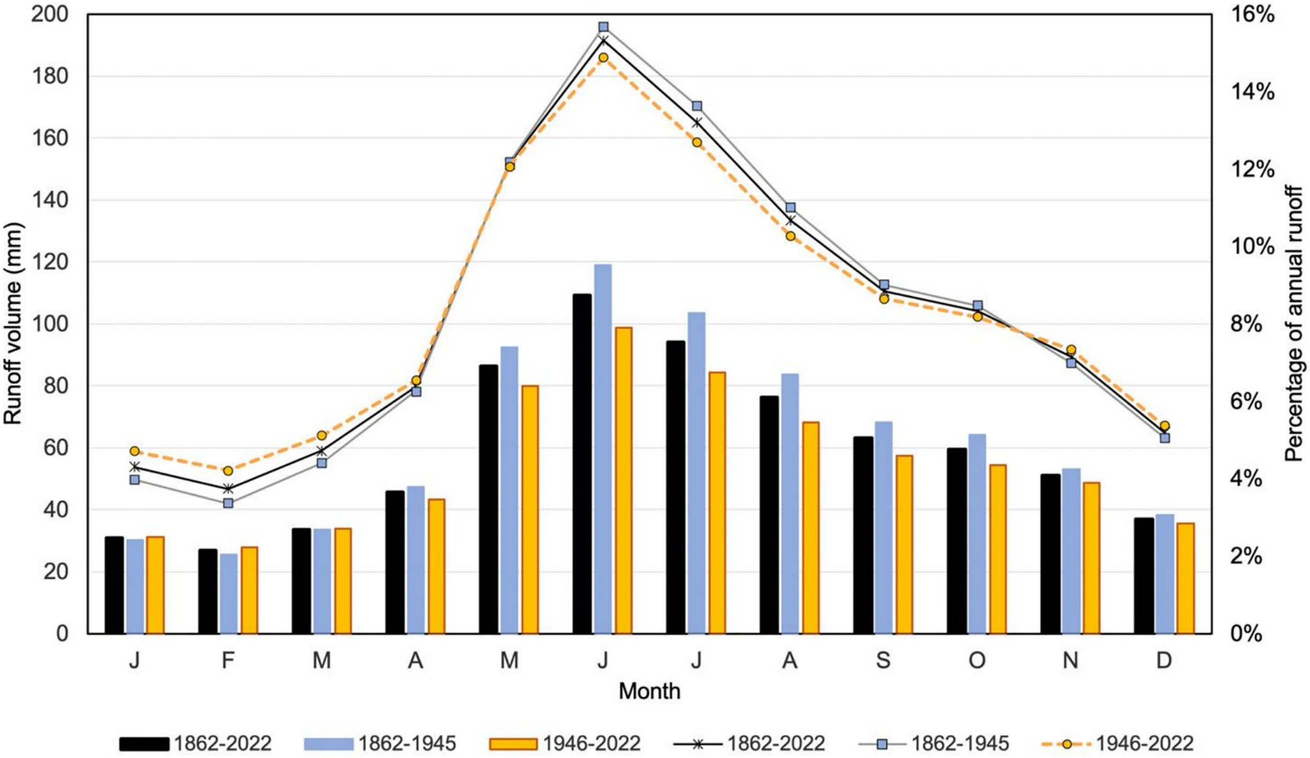

FIGURE 7 | Monthly runoff regime and percentage of mean annual runoff in the Adige river basin for the monitoring periods 1862–2022, before (1862–1945) and after (1946–2022) the construction of major reservoirs.

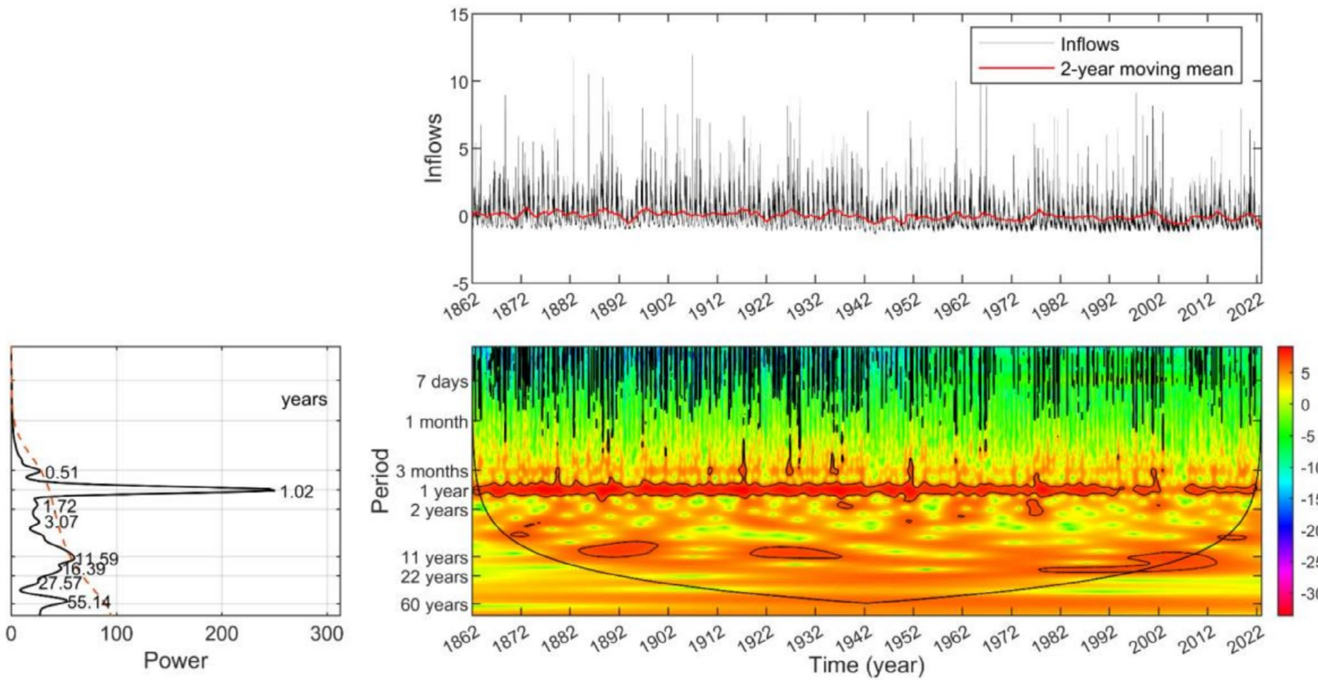

FIGURE 8 | Time series, dimensionless wavelet spectrum (bottom right) with black line indicating the limit of the Cone of Influence (COI) and the energy with 5% significance level, and global wavelet spectrum (bottom left) of daily runoff normalised; in global wavelet spectrum 5% significance levels are marked with the dashed red line.

Another spectral analysis was conducted with the wavelet coherence spectra between the streamflow series and several climatic signals at the monthly scale to assess possible teleconnections with streamflow. As shown in Figure 10 and in Figures S8 and S9, it seems that only AMO exhibits some coherence with hydrometeorological variables in the Adige river basin. Being the former a multidecadal oscillation, the coherence appears at a time scale between 11 and 30 years, and until the 1950s only, then vanishing.

10991085, 2025, 11, Downloaded from https://onlinelibrary.wiley.com/doi/10.1002/hyp.70305 by Fondazione Edmund Mach, Wiley Online Library on [03/11/2025]. See the Terms and Conditions (https://onlinelibrary.wiley.com/terms-and-conditions) on Wiley Online Library for rules of use; OA articles are governed by the applicable Creative Commons License

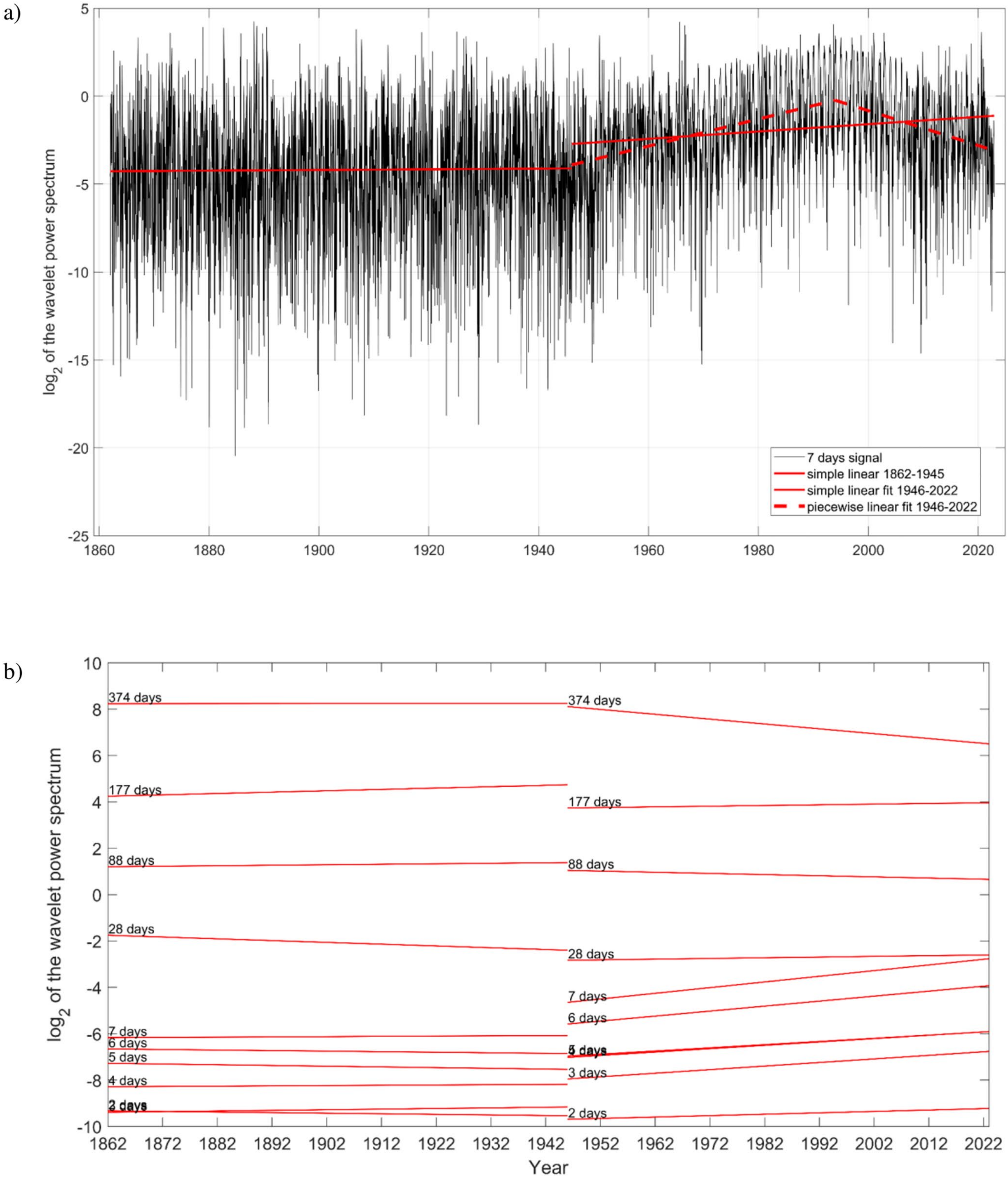

FIGURE 9 | Linear regression trends of the wavelet energy spectrum of the Adige runoff for (a) the 7-day time scale, with a piecewise linear fit for the period 1946–2022 after the construction of reservoirs and (b) at various characteristic time scales, for the periods before (1862–1945) and after (1946–2022) the construction of major reservoirs.

10991085, 2025, 11, Downloaded from https://onlinelibrary.wiley.com/doi/10.1002/hyp.70305 by Fondazione Edmund Mach, Wiley Online Library on [03/11/2025]. See the Terms and Conditions (https://onlinelibrary.wiley.com/terms-and-conditions) on Wiley Online Library for rules of use; OA articles are governed by the applicable Creative Commons License

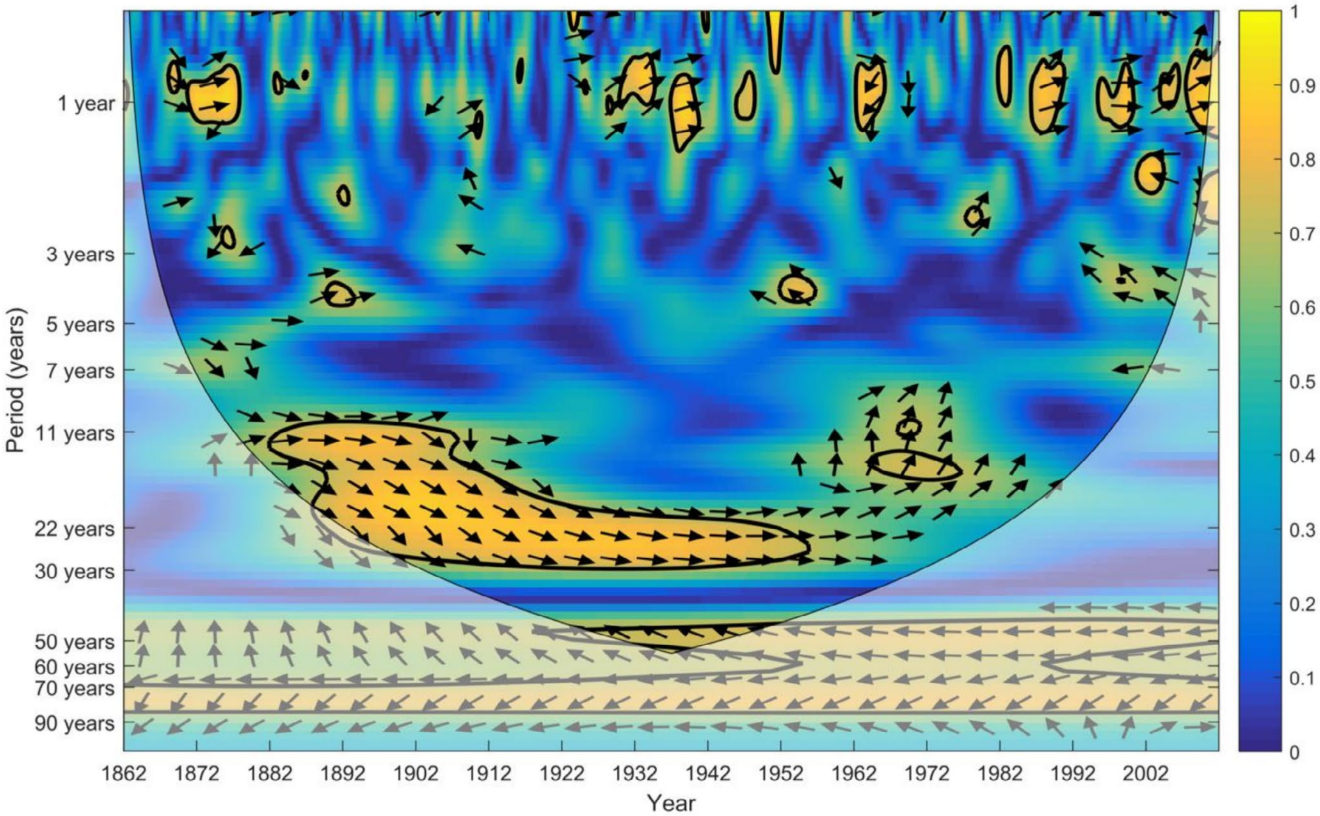

FIGURE 10 | Wavelet coherence spectrum of monthly AMO and runoff for the climatological 150-year period, 5% significance levels marked with black contour lines and COI; arrows pointing to the right indicate in-phase behaviour between the two variables, arrows pointing down indicate that the first variable anticipates the second by T/4, with T being the wavelet scale, and left-pointing arrows indicate anti-phase behaviour.

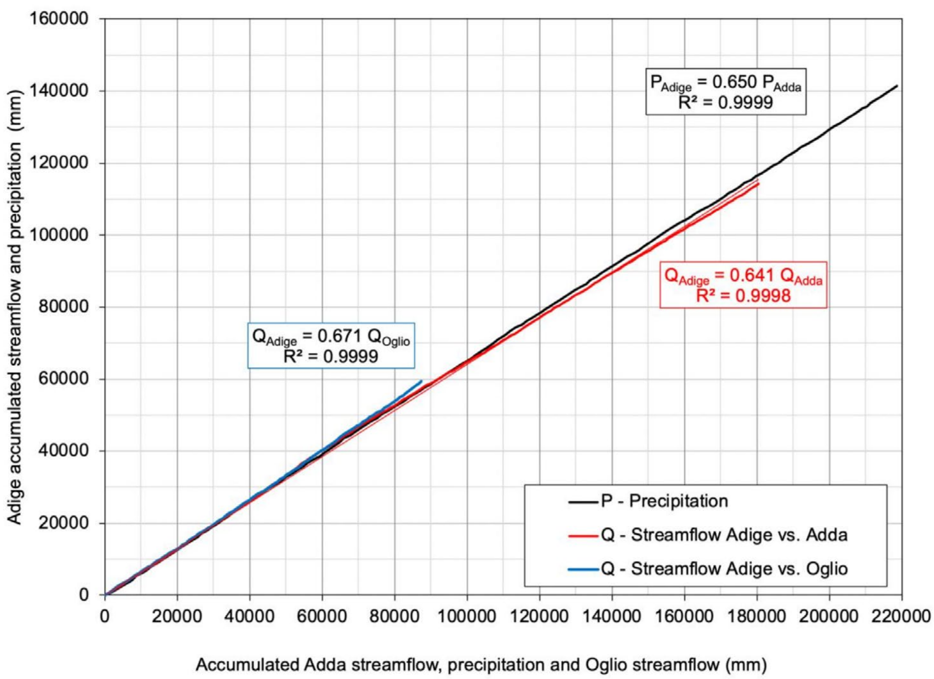

FIGURE 11 | Accumulated precipitation and streamflow for the Adige vs. Adda river basins up to the year 2022. For the Adda river, data computed by Ranzi et al. (2021) and Crespi, Matiu, et al. (2021) are reported. Accumulated streamflow is compared also for the Oglio river basin in the 1933–2022 period (Figure S10).

10991085, 2025, 11, Downloaded from https://onlinelibrary.wiley.com/doi/10.1002/hyp.70305 by Fondazione Edmund Mach, Wiley Online Library on [03/11/2025]. See the Terms and Conditions (https://onlinelibrary.wiley.com/terms-and-conditions) on Wiley Online Library for rules of use; OA articles are governed by the applicable Creative Commons License

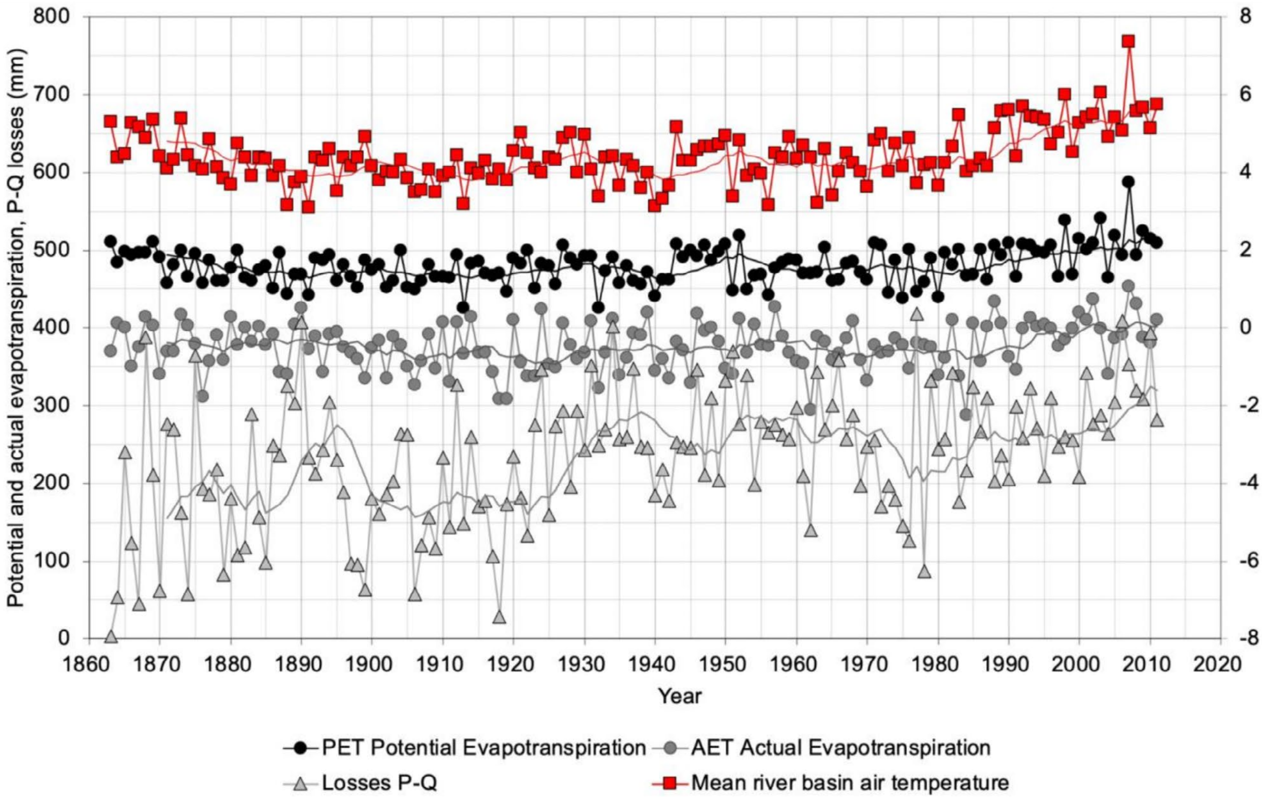

FIGURE 12 | Annual hydrological losses, potential and actual evapotranspiration, and mean temperature for the hydrological years in the period 1862–2011.

4 | Discussion

4.1 | Data Verification and Comparison With Trends in European and Alpine Rivers

From the analysis of the time series of annual streamflow, precipitation, runoff coefficient, and annual hydrological losses, as the difference between precipitation and streamflow, assuming negligible changes in the long term in the reservoirs and groundwater storage, the most evident signal is the marked decline of runoff compared to the stationarity of precipitation. As a consequence, the runoff coefficient declines, and the hydrological losses increase over time. This long-term trend is consistent with that observed by Ranzi et al. (2021) in the nearby Adda river basin and in other catchments of the central Italian Alps investigated in Ranzi et al. (2017) and in Balistrocchi et al. (2021).

Also Stahl et al. (2010), in their analysis of streamflow trends in near-natural catchments in Europe in the second half of the 1932–2004 period, found that the Mediterranean and the Danube catchments create a sort of divide between the river basins with a prevailing positive trend in the North and those with a negative one in the South. Similar results are shown in IPCC (2022) as reported in the introduction. Unfortunately, in these analyses no data are reported for the Italian basins. Montanari et al. (2023) found stationarity in the mean monthly streamflow in the Po river over the last 200 years by reconstructing 19th-century flow with the early 20th-century stage-discharge curve, an assumption that introduces uncertainty in their conclusions. Also for this reason, as a quality check and verification of our reconstruction of precipitation and streamflow time series for the Adige basin, we compared the respective double cumulative curves with those of the Adda river and the cumulative streamflow with that of the Oglio river as well (Figure 11). These river basins are close to the Adige river, at its western boundary (Figure S10). Precipitation in the Adige river basin is 65% of Adda's and, accordingly, runoff is 64%. Apart from this minor discrepancy, due to specific climatic features with a systematic minor precipitation in the Adige catchment, the agreement in the double cumulative curves is very high, for both river basins, with a coefficient of determination of the regression lines higher than 0.9998 for all the curves. In particular, the agreement is perfect for the precipitation and for the streamflow cumulative curve with Adda up to the 1910s, when the cumulative runoff exceeds 40,000 mm. Then the cumulative runoff increases in the Adige catchment just a little more rapidly than in Adda's until the 1930s, and a little less in the last decades. This is in perfect agreement with the Oglio cumulative curve for the period 1933–2022. The overall judgment on this verification check is positive and supports the reliability of our analyses.

We also compared the snow-bias corrected basin-averaged precipitation measurements with the basin-averaged uncorrected values based on up to one hundred stations' data and officially published for a 54-year period. An overall uncertainty computed

10991085, 2025, 11, Downloaded from https://onlinelibrary.wiley.com/doi/10.1002/hyp.70305 by Fondazione Edmund Mach, Wiley Online Library on [03/11/2025]. See the Terms and Conditions (https://onlinelibrary.wiley.com/terms-and-conditions) on Wiley Online Library for rules of use; OA articles are governed by the applicable Creative Commons License

with our 11 raingauge stations over a long period results in a standard error of 64 mm, being the mean in the reference official observation period of 944 mm.

As a further term of comparison, to assess the overall reliability of our reconstruction of precipitation trend based on the 11 stations analysed in Eccel and Ranzi (2025), the Adige basin-averaged precipitation estimated by Mallucci et al. (2019) in their detailed precipitation climatology for the 1956–2013 period was 912 mm, just 2.5% less than the value of 935 mm we obtained in our analysis.

Finally, as a confirmation of the decline of observed runoff in the Adige river basin, in the same paper trends over a 30-year time window exhibit a similar pattern to that shown in our Figure 5b for the Trento station; also in the upstream station of Adige at Bronzolo, gauging an area of 6926 km^2, runoff trends are mostly negative, although with low significance, throughout the 1956–2013 period, especially in summer (JJA).

4.2 | Hydrological Losses

The increase over time of 'observed' hydrological losses, L, estimated the difference between annual precipitation, P, and runoff, Q (as $L = P - Q$), is higher than the actual evapotranspiration AET estimates (Figure 12). Losses increase at a statistically significant rate of 0.86 mm $year^{-1}$ in the hydrological years, as reported in the last column of Table 2. The core of the analyses is the link between the estimated losses and those 'measured' as L. Basin-averaged temperature increased steadily over the last century at a rate of +1.2°C $century^{-1}$, accelerating in the last decades, a pattern typical of the Alps compared to the worldwide average. Potential and actual evapotranspiration increased accordingly, and their rate of increase is consistent with those simulated for the 1980–2018 period with a detailed water balance model of the Adige basin by Morlot et al. (2024), but their value systematically exceeded 'observed' losses. Possible reasons are the simplified method adopted to assess evapotranspiration or an underestimation of measured precipitation, for instance due to the well-known problem of systematic underestimation of solid precipitation which Eccel et al. (2012) found also in this region, or due to orographic effects. A second piece of evidence is the increase of the observed losses, more rapid than that of the modelled temperature-driven evapotranspirative ones, corresponding to an increase of about 30 mm over the last century, as shown by Figure 12. Considering that the observed increase of +0.86 mm $year^{-1}$ in hydrological losses corresponds to 86 mm in a century, this means that other reasons than just temperature increase must be claimed to explain such change.

Other likely causes are land-use and land-cover changes and more extensive water withdrawals for agriculture, the major source of water consumption at a global scale (Huang et al. 2018). Orchards and vineyards cover about 4.2%, and land used for agriculture, altogether, is 6.6% of the basin surface: sprinkler and drip irrigation have significantly spread in the last decades. We agree with Mallucci et al. (2019) who recognize agricultural water use as one of the possible causes for the decreased summer runoff observed in the Adige basin at Trento and Bronzolo from the 1970s onward.

Consumptive water uses of anthropic origin can be assessed based on the water balance reports issued to comply with the 2000/60/EC Water Framework Directive. In these reports, water withdrawals authorised for agriculture assessed at the scale of the Adige basin (in Figure 1 together with its main tributaries), covering an area of 7375 km^2, correspond to 4.71 m^3s^{-1} (Provincia Autonoma di Bolzano 2017); those for the Noce river tributary (1367 km^2) correspond to 4.47 m^3s^{-1} and those for the Avisio river tributary (940 km^2) to 1.27 $m^3 s^{-1}$ on average in a year (Provincia Autonoma di Trento 2012). Considering the small portion of the Adige river just upstream the Trento gauging station, agricultural water uses, based on the mean annual authorised withdrawals, correspond to 10.7 $m^3 s^{-1}$ that is, 34.8 mm $year^{-1}$ of specific runoff at the scale of the Adige catchment in Trento, and are concentrated in the months of April to September with a peak of 25 $m^3 s^{-1}$ in June. Such intensive use for agriculture only started in the second half of the 20th century. Other consumptive uses for civil and industrial purposes were assessed, based on the data in the same reports and assuming an effective loss of 20% of the withdrawn volume, as 1.0 $m^3 s^{-1}$ that is, 3.3 mm $year^{-1}$. We can argue that 38 mm $century^{-1}$ that is, about 44% of the observed hydrological losses in the last century, could be attributed to anthropic water withdrawals. These would reach 40 mm if the effective loss for civil and industrial uses were 40% of the withdrawn volume, a reasonable upper limit.

Another possible cause of runoff decline can be attributed to land-use and land-cover changes. Meadows and pastures cover an additional 25% of the basin surface and forests 62%. With such relevant areas contributing to evapotranspiration, it is reasonable to conjecture that land use changes over the last two centuries have induced changes also in hydrological losses. Ranzi et al. (2017) analysed four cadastral maps, each covering an area of 11.5 km^2, dating back to the mid-19th century in the Adige river basin, representative of urban, forested, and agricultural areas. Past land use was compared with the present one, and in all areas, with the exception of the urban ones, a dramatic increase in forest cover was observed (Tudoroiu et al. 2016). The same land-use dynamics, consistent with the widespread afforestation that has been occurring in Europe over the last decades (FAO 2024), were observed by comparing land-use changes in the nearby Oglio river basin by Balistrocchi et al. (2021). These land-use and land-cover changes could explain the remaining 17 mm $year^{-1}$ of the 86 mm of hydrological losses observed in the last century.

A more comprehensive and extensive analysis of the combined effect of changes in land use, temperature rise, and irrigation practices on evapotranspiration losses is envisaged as a research perspective, but it is very reasonable to assume that part of the enhanced hydrological losses is due to the higher evapotranspiration rates resulting from these three factors: temperature increase, enhanced water withdrawals for irrigation and anthropic uses, and afforestation.

10991085, 2025, 11, Downloaded from https://onlinelibrary.wiley.com/doi/10.1002/hyp.70305 by Fondazione Edmund Mach, Wiley Online Library on [03/11/2025]. See the Terms and Conditions (https://onlinelibrary.wiley.com/terms-and-conditions) on Wiley Online Library for rules of use; OA articles are governed by the applicable Creative Commons License

A consequence is that hydrological droughts are more severe than the meteorological ones. The visual inspection of Figure 5a clearly indicates that the severity of the meteorological droughts, estimated in terms of 10-year moving average, of the 1940s, 1970s, and early 2000s is comparable, the latter being the less severe of the three. The hydrological drought of the 2000s, instead, was the most severe (Figure 5b), also because of the more marked losses.

Another land cover change that has influenced changes in the streamflow regimes is the glacier retreat observed in the Alps since the end of the Little Ice Age in the mid-19th century, with a more marked intensity in the central Italian Alps (Grossi et al. 2013; Carturan et al. 2016). The rate of mass balance loss accelerated in the last four decades and also the extent of the ice cover, so that the contribution of additional runoff volume provided by glaciers' melt needs a specific investigation for a more thorough attribution analysis.

4.3 | Reasons for the Changes in Monthly Precipitation and Runoff Regimes

The shift in the monthly distribution of runoff was influenced not only by climatic changes but also by the effect of reservoirs, as their specific storage capacity of 58.5 mm corresponds to about 8% of the annual runoff volume. The precipitation decrease in March is compensated by the water release from reservoirs in the winter and early spring period, when the cost of energy and the revenues from hydropower generation were generally higher, especially until the beginning of the present century, when the more widespread use of air conditioning

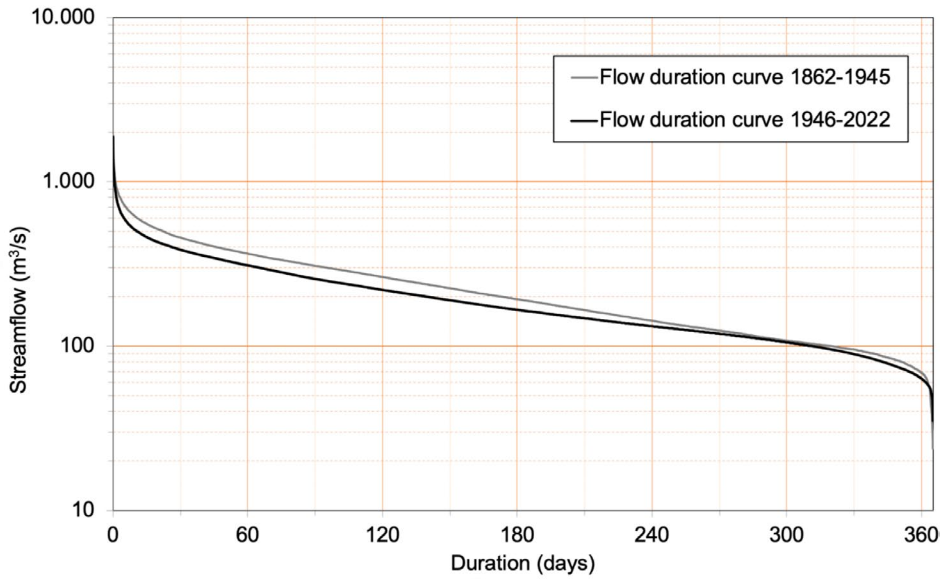

FIGURE 13 | Flow duration curves for the observation periods before and after the completion of the major reservoirs.

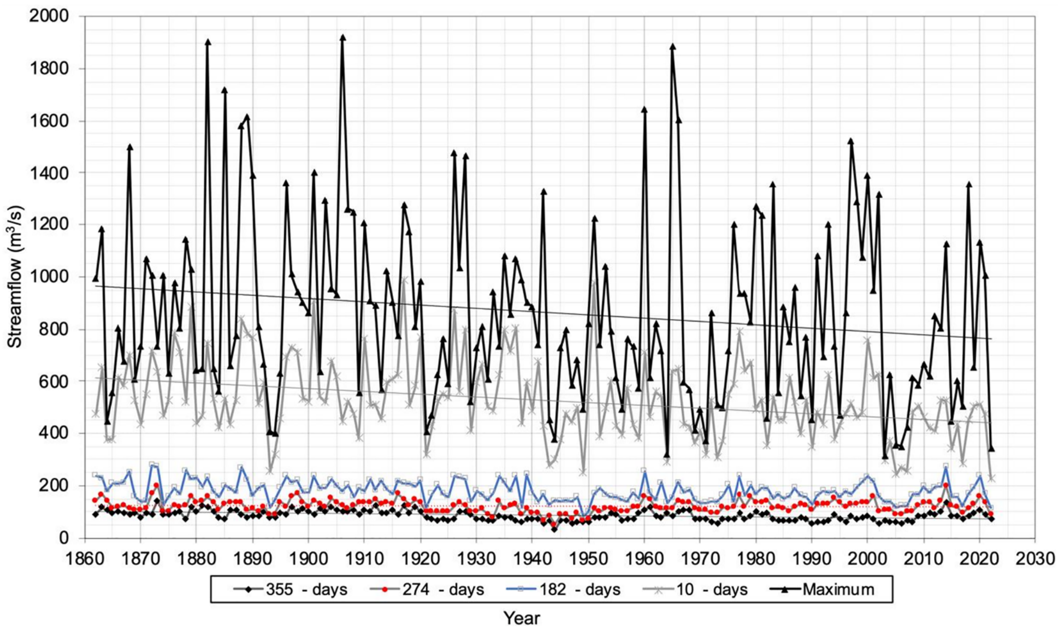

FIGURE 14 | Indices of streamflow with durations of 355, 274, 182, 10 and annual maxima of daily flows.

10991085, 2025, 11, Downloaded from https://onlinelibrary.wiley.com/doi/10.1002/hyp.70305 by Fondazione Edmund Mach, Wiley Online Library on [03/11/2025]. See the Terms and Conditions (https://onlinelibrary.wiley.com/terms-and-conditions) on Wiley Online Library for rules of use; OA articles are governed by the applicable Creative Commons License

systems and the market of energy changed remarkably and impacted the reservoirs management. It is likely that the statistically significant runoff increase in the winter period (Table S3) is mainly due to the artificial storages' practices for hydropower generation. In fact, according to data reported by the National Civil Protection Agency, in the 1996–2022 period, specific water volumes released from reservoirs in the Adige river basin in the winter period DJFM correspond to over 12 mm, a value consistent with the sign of the observed trend and the changes in runoff prior to and after 1946 (Table S3). A second possible cause, as noticed by Mallucci et al. (2019) and Napoli et al. (2025), is the increased aquifer recharge in the autumn, consistent with increased precipitation in the same period. Volumes stored in reservoirs in MJJA correspond to over 18 mm, a value consistent with the sign of the observed trend and the changes in runoff prior to and after 1946 (Table S3), although not capable of explaining the entire difference. The significant decrease in summer runoff (JJA) after 1945 (Figures S6, S7 and Table S3) at a rate of $-0.647\,\mathrm{mm\,year^{-1}}$ can be explained by: (i) the water storage in reservoirs during the high-flow months but also by (ii) the enhanced evapotranspiration losses induced by higher temperatures and irrigation withdrawals; (iii) the anticipated spring snowmelt induced by the higher temperatures and the diminished SWE in early spring as indicated by statistics in the Adige basin presented by Marcolini et al. (2017) and, in SWE climatology analyses in the Italian Alps after 1967, by Ranzi et al. (2024), and in 1930–2020 by Colombo et al. (2022). The autumn (SON) runoff increase in the last decades at a rate of $0.229\,\mathrm{mm\,year^{-1}}$, instead, is a result of the precipitation increase in that season, at a rate of $0.465\,\mathrm{mm\,year^{-1}}$. These rates of change, however, are not statistically significant. A similar shift in the runoff monthly distribution before and after the reservoir construction was observed for the Adda river basin, and, more remarkably, as the specific volume of reservoirs in that catchment is 114 mm, more than 10% of the annual runoff (Ranzi et al. 2021).

A minor cause of the increased observed hydrological losses is the $19.27\,\mathrm{km^2}$ increase of the lakes' surface introduced by artificial reservoirs. For the Molveno lake, close to the boundary of the Adige river basin, evaporation was estimated by Tonini (1983) in the range of about $800\,\mathrm{mm\,year^{-1}}$ at 823 m asl, higher than evapotranspiration from forests and agricultural areas, but whose net effect on the water balance can be estimated in additional losses of about $1\,\mathrm{mm\,year^{-1}}$.

4.4 | Possible Causes of Variability of Spectral Properties

Figure 9 can clearly and interestingly highlight anthropic influences on the streamflow regime. In the top panel, the energy at the 7-day time scale is shown together with the trendlines fitted before and after 1945, when the construction of reservoirs accelerated (Table 1 and Figure S1). The patterns and trends in Figure 9a are consistent with the weekly regulation of reservoirs to adapt to the minor energy demand and cost on the weekends. The energy signal appears to be stationary in the first period, when 'natural' conditions prevailed. After 1945, instead, energy at the weekly scale increases steadily until the end of the century, then declines again. At that time, policies started to be legally binding in fostering more natural regimes in streams and coping with the 'environmental flow' (Majone et al. 2016), limiting the effect of the so-called 'hydropeaking' (Zolezzi et al. 2009). The increasing intensity at the 3- to 7-day scale after the construction of reservoirs was a result of hydropower regulation, as well as the decrease of energy at the annual scale because of the long-term runoff volume decline (Figure 9b).

In the top panel of this figure, a continuous piecewise linear fit was performed after the 1945 change point. Energy in the 7-day scale component of the wavelet spectrum rapidly increases until the late 1990s, declining later. We interpret this behaviour as an effect of non-regulated exploitation of water resources for hydropower generation in the early decades, eventually mitigated by the introduction of more stringent environmental standards. In the 2010s, the energy resumes almost constant values closer to the natural conditions prior to the 1940s. This result is an example of non-stationarity identified in time series and of its likely causes, in this case the anthropic ones, introduced by environmental legislation (Law 183/1989, Decrees 275/1993, 463/1999, 152/2006).

The evidence of an energy decrease in the coherence spectrum between streamflow and AMO, observed in Section 3.4, seems to be not an effect of climatic changes on teleconnections, such a decrease not being observable in the coherence of precipitation with AMO at the same time scale (Eccel and Ranzi 2025). In our opinion, it can be also attributed to the effect of the reservoirs, completed, indeed, after the 1950s and that introduced an artificial time shift in the runoff.

4.5 | Flow Duration Curve, Low and High Flow Changes

The flow duration curves computed for the two observation periods are represented in Figure 13. A streamflow decrease is evident for all durations, ranging from low flows, 355 days long, to the daily annual maxima (Figure 14 and Table S2). The observed decline of annual maxima, with a Theil–Sen slope of the regression line of $-1.27\,\mathrm{m^3\,s^{-1}\,year^{-1}}$ (and a Mann-Kendall $Z = -2.27$), is both the effect of an uncommon series of severe floods with daily flow above $1500\,\mathrm{m^3\,s^{-1}}$ with six exceedances occurring in the first 50-year period (1868, 1882, 1885, 1888, 1889, and 1906), just one in the following five decades, and two in the last 61 years, and a result of the positive effects of reservoirs in storing runoff volumes during floods, after the 1940s, for instance during the 1966 'century flood' (Dorigo 1967; Malguzzi et al. 2006). Our result is consistent with the slight declining trend of the 172-year time series of maximum daily floods observed for the Adda river (Ranzi et al. 2021). Although the focus of this paper is not on extreme floods, the result about annual maxima of daily streamflow may appear in disagreement with the common perception of a widespread increase in flood intensity, but is consistent with the detailed analyses on trends of maximum flows in the 1960–2010 period, exhibiting variable patterns in Europe, conducted by Blöschl et al. (2017, 2019). In those studies, the Alpine mountain divide is a sort of boundary between the region with increasing floods in the north and decreasing ones in the south. This result points out the relevance of reconstructing and analysing long time series, as the one of daily streamflow maxima,

10991085, 2025, 11, Downloaded from https://onlinelibrary.wiley.com/doi/10.1002/hyp.70305 by Fondazione Edmund Mach, Wiley Online Library on [03/11/2025]. See the Terms and Conditions (https://onlinelibrary.wiley.com/terms-and-conditions) on Wiley Online Library for rules of use; OA articles are governed by the applicable Creative Commons License

also for the estimation of long-recurrence intervals in flood frequency analysis.

Worth noticing is the fact that after the year 2000, when water authorities paid more attention to the environmental quality of the river systems, the 355-day duration streamflow rose steadily above 50 $m^3 s^{-1}$, a value that was never exceeded in several years before (Figure 14).

5 | Conclusions

The second-longest, so far unpublished, time series of daily water level and streamflow data available for Italian rivers is reconstructed, spanning over 161 years (1862–2022). This enabled the identification of patterns of variability and changes in the streamflow regime in a well-monitored mountain area and to attribute to natural and man-induced forcings the reasons for such changes.

- Annual runoff decline occurred at a statistically significant rate of −1.01 mm $year^{-1}$ and −1.4% $decade^{-1}$ from the series start and was faster than precipitation decrease (19 mm $century^{-1}$, statistically non-significant), a result consistent with the observations in the nearby Adda basin.
- A 5% significance change point in annual runoff was detected with the Pettitt test just before the 1940s dry period, without any corresponding change in precipitation, another result consistent with the hydrometric and precipitation observations for the Adda river.
- When testing the potential influence of large-scale climatic indices such as NAO, WeMO, and AMO on streamflow, we found that statistically significant teleconnections of hydrometeorological variables only appear with AMO and only before the completion of reservoirs, which are causes of disruption of the natural streamflow regime.
- Other changes in the runoff regime may be attributed to the anthropic influence of reservoirs, such as the relative increase in JFM due to hydropower generation and a decrease in JJA percentage of the annual runoff due to water storage.
- Another effect of hydropower reservoirs is the increase of energy in the high-frequency spectrum at daily to weekly scales observed after their construction.
- The attention paid in the last two decades by water authorities to the conservation of environmental flow was effective in re-establishing more natural conditions in the spectrum of short-duration fluctuations, as well as in the low-duration flow.
- The daily streamflow decline is observed for all durations of the flow duration curve including the annual maxima, with a significant decrease at a rate of −1.27 $m^3 s^{-1} year^{-1}$, likely because of a combined effect of a series of floods that occurred in the second half of the 19th century and the construction of reservoirs in the last century.
- The observed increase of hydrological losses (86 mm $century^{-1}$), especially in summer, can be explained in terms of more intensive water withdrawals (38 mm $century^{-1}$), mainly for irrigation since the second half of the last century, enhanced evapotranspiration losses due to temperature increase (30 mm $century^{-1}$), and afforestation (17 mm $century^{-1}$).
- The impact of the 19.27 km^2 increase of artificial lakes' surface is negligible, contributingapproximately 1 mm $century^{-1}$ of water losses.

Acknowledgements

The first author thanks the Po River District Basin Authority for its partial support of this research through grant no. 8536/2020. The Archive of the Trento Municipality made accessible the manuscripts of the readings of the daily water level data conducted from 1862 until 1927. Provincia Autonoma di Trento (PAT) is thanked for having made available stage-discharge curves and hydrometric data after 1975 (see also http://www.floods.it/public/). Precipitation and temperature data were made available by PAT and Provincia Autonoma di Bolzano. R.R. contributed to the hydrometric data collection and processing, the conceptualization of the paper, writing, and reviewing; E.E. to the meteorological data collection and processing, writing, and reviewing. P.C. contributed to the development and processing of the MARTA triangles, Figures 1 and 9a generation and reviewing; EM conducted the wavelet spectral analysis. Matteo Balistrocchi is thanked for having improved Figure S1. The wavelet spectral analysis made use of the software developed by C. Torrence and G. Compo, freely available at http://paos.colorado.edu/research/wavelets/, and, for the coherence spectra, by A. Grinsted, J. Moore, and S. Jevrejeva at http://grinsted.github.io/wavelet-coherence/. Two anonymous reviewers are thanked for their useful suggestions. Open access publishing facilitated by Universita degli Studi di Brescia, as part of the Wiley - CRUI-CARE agreement.

Data Availability Statement

Hydrometric level data originally collected in this study for the 1862–1919 period, streamflow data reconstructed for the 1862–1922 period, and hydrometric data already available with open access will be shared on scientific data repositories with public access upon the publication acceptance of this paper. Hydrometric data and visualisation packages data are accessible on demand from the public repository of the University of Brescia IRIS OPENBS https://hdl.handle.net/11379/630565 and meteorological data at the link https://iris.unibs.it/handle/11379/626785.

References

Albertelli, M. 2014. *Idrometria dell'Adige a Trento dal 1862 al 2011 in Relazione agli Interventi Antropici ed alle Variazioni del Clima [Unpublished master dissertation]*. University of Brescia.

Apollonio, A. 1885. *Relazione sulle Piene dell'Adige e dell'Avisio e Sui Lavori da Eseguirsi per Difendere la Città e le Campagne di Trento*. Vol. 29, 1–20. Marietti.

Auer, I., R. Böhm, A. Jurkovic, et al. 2007. "HISTALP—Historical Instrumental Climatological Surface Time Series of the Greater Alpine Region." *International Journal of Climatology* 27: 17–46. https://doi.org/10.1002/joc.1377.

Balistrocchi, M., M. Tomirotti, A. Muraca, and R. Ranzi. 2021. "Hydroclimatic Variability and Land Cover Transformations in the Central Italian Alps." *Water* 13, no. 7: 963. https://doi.org/10.3390/w13070963.

Beniston, M., H. F. Diaz, and R. S. Bradley. 1997. "Climatic Change at High Elevation Sites: An Overview." *Climatic Change* 36: 233–251. https://doi.org/10.1023/A:1005380714349.

10991085, 2025, 11, Downloaded from https://onlinelibrary.wiley.com/doi/10.1002/hyp.70305 by Fondazione Edmund Mach, Wiley Online Library on [03/11/2025]. See the Terms and Conditions (https://onlinelibrary.wiley.com/terms-and-conditions) on Wiley Online Library for rules of use; OA articles are governed by the applicable Creative Commons License

Bierkens, M. F. P., and L. P. H. van Beek. 2009. “Seasonal Predictability of European Discharge: NAO and Hydrological Response Time.” *Journal of Hydrometeorology* 10: 953–968. https://doi.org/10.1175/2009JHM1034.1.

Blöschl, G., J. Hall, J. Parajka, et al. 2017. “Changing Climate Shifts Timing of European Floods.” *Science* 357, no. 6351: 588–590.

Blöschl, G., J. Hall, A. Viglione, et al. 2019. “Changing Climate Both Increases and Decreases European River Floods.” *Nature* 573: 108–111.

Brugnara, Y., and M. Maugeri. 2019. “Daily Precipitation Variability in the Southern Alps Since the Late 19th Century.” *International Journal of Climatology* 39, no. 8: 3492–3504. https://doi.org/10.1002/joc.6034.

Brunetti, M., G. Lentini, M. Maugeri, et al. 2009. “Climate Variability and Change in the Greater Alpine Region Over the Last Two Centuries Based on Multi- Variable Analysis.” *International Journal of Climatology* 29: 2197–2225.

Carturan, L., C. Baroni, M. Brunetti, et al. 2016. “Analysis of the Mass Balance Time Series of Glaciers in the Italian Alps.” *Cryosphere* 10: 695–712. https://doi.org/10.5194/tc-10-695-2016.

Ceola, S., A. Montanari, T. Krueger, et al. 2016. “Adaptation of Water Resources Systems to Changing Society and Environment: A Statement by the International Association of Hydrological Sciences.” *Hydrological Sciences Journal* 61, no. 16: 2803–2817.

Chiu, C. L. 1988. “Entropy and 2-D Velocity Distribution in Open Channels.” *Journal of Hydraulic Engineering* 114, no. 7: 738–756.

Colombo, M. 2016. *Ricostruzione ed analisi statistica della serie storica delle precipitazioni di Cavalese dal 1882 al 2011 [Degree Dissertation in Civil Engineering].* University of Brescia (in Italian).

Colombo, N., M. Valt, E. Romano, et al. 2022. “Long-Term Trend of Snow Water Equivalent in the Italian Alps.” *Journal of Hydrology* 614: 128532. https://doi.org/10.1016/j.jhydrol.2022.128532.

Crespi, A., M. Brunetti, R. Ranzi, M. Tomirotti, and M. Maugeri. 2021. “A Multi-Century Meteo-Hydrological Analysis for the Adda River Basin (Central Alps). Part I: Gridded Monthly Precipitation (1800–2016) Records.” *International Journal of Climatology* 41, no. 1: 162–180. https://doi.org/10.1002/joc.6614.

Crespi, A., M. Matiu, G. Bertoldi, M. Petitta, and M. Zebisch. 2021. “A High-Resolution Gridded Dataset of Daily Temperature and Precipitation Records (1980–2018) for Trentino-South Tyrol (North-Eastern Italian Alps).” *Earth System Science Data* 13: 2801–2818. https://doi.org/10.5194/essd-13-2801-2021.

Di Baldassarre, G., and A. Montanari. 2009. “Uncertainty in River Discharge Observations: A Quantitative Analysis.” *Hydrology and Earth System Sciences* 13, no. 6: 913–921.

Dorigo, K. 1967. *La Piena dell'Adige del novembre 1966 con brevi cenni alle precedenti piene*. Ufficio Idrografico del Magistrato delle Acque, Ministero dei Lavori Pubblici-Servizio Idrografico.

Eccel, E., E. Cordano, F. Zottele, and G. B. Toller. 2015. “ClimClass and ClimClassMap: Two R- Packages for Climatic and Agro-Bioclimatic Indices. An Application to Trentino.” In *Proceedings of the 18th National Congress of Agrometeorology, 9th-11th June 2015, San Michele All'adige (I Book of Extended Abstract).* AIAM.

Eccel, E., and R. Ranzi. 2025. *Climate Variability for a 150-Year (1862–2011).* Water Balance Series in the Italian Alps at Different Time Scales.

FAO. 2024. *The State of the World's Forests*. Food and Agriculture Organisation of the United Nations.

Eccel, E., P. Cau, and R. Ranzi. 2012. “Data Reconstruction and Homogenization for Reducing Uncertainties in High-Resolution Climate Analysis in Alpine Regions.” *Theoretical and Applied Climatology* 110: 345–358. https://doi.org/10.1007/s00704-012-0624-z.

Gaudard, L., F. Romerio, F. Dalla Valle, et al. 2014. “Climate Change Impacts on Hydropower in the Swiss and Italian Alps.” *Science of the Total Environment* 493: 1211–1221. https://doi.org/10.1016/j.scitotenv.2013.10.012.

Gobiet, A., S. Kotlarski, M. Beniston, G. Heinrich, J. Rajczak, and M. Stoffel. 2014. “21st Century Climate Change in the European Alps—A Review.” *Science of the Total Environment* 493: 1138–1151.

GRDC. 2021. *Adda River Streamflow Data (Data Set).* Global Runoff Data Center. https://www.bafg.de/GRDC/EN/Home/homepage_node.html.

Grossi, G., P. Caronna, and R. Ranzi. 2013. “Hydrologic Vulnerability to Climate Change of the Mandrone Glacier (Adamello-Presanella Group, Italian Alps).” *Advances in Water Resources* 55: 190–203. https://doi.org/10.1016/j.advwatres.2012.11.014.

Grossi, G., A. Lendvai, G. Peretti, and R. Ranzi. 2017. “Snow Precipitation Measured by Gauges: Systematic Error Estimation and Data Series Correction in the Central Italian Alps.” *Water* 9, no. 7: 461. https://doi.org/10.3390/w9070461.

Hasson, S., J. Böhner, and V. Lucarini. 2017. “Prevailing Climatic Trends and Runoff Response From Hindukush–Karakoram–Himalaya, Upper Indus Basin.” *Earth System Dynamics* 8: 337–355. https://doi.org/10.5194/esd-8-337-2017.

Hosking, J. R. M., and J. R. Wallis. 1997. *Regional Frequency Analysis: An Approach Based on L-Moments*. Cambridge University Press.

Huang, Z., M. Hejazi, X. Li, et al. 2018. “Reconstruction of Global Gridded Monthly Sectoral Water Withdrawals for 1971–2010 and Analysis of Their Spatiotemporal Patterns.” *Hydrology and Earth System Sciences* 22: 2117–2133. https://doi.org/10.5194/hess-22-2117-2018.

Hurrell, J. W., Y. Kushnir, G. Ottersen, and M. Visbeck, eds. 2003. *The North Atlantic Oscillation: Climatic Significance and Environmental Impact. Geophysical Monograph*. American Geophysical Union.

IPCC. 2022. “Climate Change 2022: Impacts, Adaptation and Vulnerability.” In *Contribution of Working Group II to the Sixth Assessment Report of the Intergovernmental Panel on Climate Change*, edited by H. O. Pörtner, D. C. Roberts, M. Tignor, et al., 3056. Cambridge University Press. https://doi.org/10.1017/9781009325844.

Kommission bei W. Braumüller. 1903. *Hydrographischer Dienst in Österreich (1893–1912). Jahrbuch des k.k. Hydrographschen Centralbureaus. Das Etsch Gebiet*. k. k. Hof - und Universitäts-Buchhändler.

Liaqat, M. U., G. Grossi, S. U. Hasson, and R. Ranzi. 2022. “Characterization of Interannual and Seasonal Variability of Hydro-Climatic Trends in the Upper Indus Basin.” *Theoretical and Applied Climatology* 147: 1163–1184. https://doi.org/10.1007/s00704-021-03850-3.

Majone, B., F. Villa, R. Deidda, and A. Bellin. 2016. “Impact of Climate Change and Water Use Policies on Hydropower Potential in the Southeastern Alpine Region.” *Science of the Total Environment* 543: 965–980. https://doi.org/10.1016/j.scitotenv.2015.05.009.

Malguzzi, P., G. Grossi, A. Buzzi, R. Ranzi, and R. Buizza. 2006. “The 1966 ‘Century’ Flood in Italy: A Meteorological and Hydrological Revisitation.” *Journal of Geophysical Research: Atmospheres* 111: D24106. https://doi.org/10.1029/2006JD007111.

Mallucci, S., B. Majone, and A. Bellin. 2019. “Detection and Attribution of Hydrological Changes in a Large Alpine River Basin.” *Journal of Hydrology* 575: 1214–1229. https://doi.org/10.1016/j.jhydrol.2019.06.020.

Marcolini, G., A. Bellin, M. Disse, and G. Chiogna. 2017. “Variability in Snow Depth Time Series in the Adige Catchment.” *Journal of Hydrology: Regional Studies* 13: 240–254. https://doi.org/10.1016/j.ejrh.2017.08.007.

10991085, 2025, 11, Downloaded from https://onlinelibrary.wiley.com/doi/10.1002/hyp.70305 by Fondazione Edmund Mach, Wiley Online Library on [03/11/2025]. See the Terms and Conditions (https://onlinelibrary.wiley.com/terms-and-conditions) on Wiley Online Library for rules of use; OA articles are governed by the applicable Creative Commons License

Marzeion, B., and A. Nesje. 2012. "Spatial Patterns of North Atlantic Oscillation Influence on Mass Balance Variability of European Glaciers." *Cryosphere* 6: 661–673. https://doi.org/10.5194/tc-6-661-2012.

Montanari, A., and D. Koutsoyiannis. 2014. "Modeling and Mitigating Natural Hazards: Stationarity is Immortal!" *Water Resources Research* 50: 9748–9756. https://doi.org/10.1002/2014WR016092.

Montanari, A., H. Nguyen, S. Rubinetti, et al. 2023. "Why the 2022 Po River Drought is the Worst in the Past Two Centuries. Science." *Advances* 9, no. 32: eadg8304. https://doi.org/10.1126/sciadv.adg8304.

Moramarco, T., C. Saltalippi, and V. P. Singh. 2004. "Estimation of Mean Velocity in Natural Channels Based on Chiu's Velocity Distribution Equation." *Journal of Hydrologic Engineering* 9, no. 1: 42–50.

Morlot, M., R. Rigon, and G. Formetta. 2024. "Hydrological Digital Twin Model of a Large Anthropized Italian Alpine Catchment: The Adige River Basin." *Journal of Hydrology* 629: 130587. https://doi.org/10.1016/j.jhydrol.2023.130587.

Municipio di Trento. 1889. *Relazione Sull'efficacia dei Lavori Recentemente Eseguiti ed Ancor da Eseguirsi Lungo l'Adige a Difesa della Città e delle Campagne di Trento (A Cura di A. Apollonio)*, 1–9. L. T. Scotoni e Vitti.

Napoli, A., M. Matiu, L. Laiti, et al. 2025. "Review on Climate Change Impacts on the Water-Energy-Food-Ecosystems (WEFE) Nexus in the North-Eastern Italian Alps." *Climatic Change* 178, no. 3: 41. https://doi.org/10.1007/s10584-025-03890-y.

Noto, L. V., G. Cipolla, D. Pumo, and A. Francipane. 2023. "Climate Change in the Mediterranean Basin (Part II): A Review of Challenges and Uncertainties in Climate Change Modeling and Impact Analyses." *Water Resources Management* 37: 2307–2323. https://doi.org/10.1007/s11269-023-03444-w.

Otto, F., G. van Oldenborgh, J. Eden, P. A. Stott, D. J. Karoply, and M. R. Allen. 2016. "The Attribution Question." *Nature Climatic Change* 6: 813–816.

Provincia Autonoma di Trento. 2012. Aggiornamento del Bilancio Idrico Provinciale. http://osservatorio.energia.provincia.tn.it/bilanci_idrici/aspetti%20quantit%c3%a0%20APRIE/.

Provincia Autonoma di Trento. 2015. *Progetto di Piano di Gestione del Rischio Alluvioni della Provincia Autonoma di Trento*. Provincia Autonoma di Trento.

Provincia Autonoma di Bolzano - Alto Adige. 2017. *Piano Generale di Utilizzazione delle Acque Pubbliche (in Italian, available also in German)*. Provincia Autonoma di Bolzano - Alto Adige.

Provincia Autonoma di Trento, Ufficio Idrografico. 1978. "Annali Idrologici (Hydrological Yearbooks), Year 1975 (In Italian)." *Calliano*: 153.

R Core Team. 2025. *R: A Language and Environment for Statistical Computing*. R Foundation for Statistical Computing. https://www.r-project.org/.

Ranzi, R., E. Michailidi, M. Tomirotti, A. Crespi, M. Brunetti, and M. Maugeri. 2021. "A Multi-Century Meteo-Hydrological Analysis for the Adda River Basin (Central Alps). Part II: Daily Runoff (1845–2016) at Different Scales." *International Journal of Climatology* 41, no. 1: 181–199. https://doi.org/10.1002/joc.6678.

Ranzi, R., P. Caronna, and M. Tomirotti. 2017. "Impact of Climatic and Land Use Changes on River Flows in the Southern Alps." In *Sustainable Water Resources Planning and Management Under Climate Change*, edited by E. Kolokytha, O. Satoru, and R. S. V. Teegavarapu, 61–83. Springer.

Ranzi, R., P. Colosio, and G. Galeati. 2024. "Climatology of Snow Depth and Water Equivalent Measurements in the Italian Alps (1967–2020)." *Hydrology and Earth System Sciences* 28: 2555–2578. https://doi.org/10.5194/hess-28-2555-2024.

Rotach, M. W., P. Ambrosetti, F. Ament, et al. 2009. "MAP D-PHASE: Real-Time Demonstration of Weather Forecast Quality in the Alpine Region." *Bulletin of the American Meteorological Society* 90, no. 9: 1321–1336. https://doi.org/10.1175/2009BAMS2776.1.

Schaefli, B., B. Hingray, and A. Musy. 2007. "Climate Change and Hydropower Production in the Swiss Alps: Quantification of Potential Impacts and Related Modelling Uncertainties." *Hydrology and Earth System Sciences* 11: 1191–1205. https://doi.org/10.5194/hess-11-1191-2007.

Scolozzi, R., and E. Eccel. 2017. "Gli Esordi della Meteorologia in Trentino Nelle fonti d'Archivio tra Otto e Novecento." *Archivio Trentino* 2017, no. 1: 246–311.

Singh, A., P. J. Sharma, and R. S. Teegavarapu. 2024. "Understanding Non-Stationarity Patterns in Basin-Scale Hydroclimatic Extremes." *International Journal of Climatology* 44: 3867–3887. https://doi.org/10.1002/joc.8557.

Smiraglia, C., and G. Diolaiuti. 2015. *The New Italian Glacier Inventory*, 400. Ev-K2-CNR.

Stahl, K., H. Hisdal, J. Hannaford, et al. 2010. "Streamflow Trends in Europe: Evidence From a Dataset of Near-Natural Catchments." *Hydrology and Earth System Sciences* 14: 2367–2382. https://doi.org/10.5194/hess-14-2367-2010.

Steirou, E., L. Gerlitz, H. Apel, and B. Merz. 2017. "Links Between Large-Scale Circulation Patterns and Streamflow in Central Europe: A Review." *Journal of Hydrology* 549: 484–500. https://doi.org/10.1016/j.jhydrol.2017.04.003.

Su, L., C. Miao, D. Kong, et al. 2018. "Long-Term Trends in Global River Flow and the Causal Relationships Between River Flow and Ocean Signals." *Journal of Hydrology* 563: 818–833. https://doi.org/10.1016/j.jhydrol.2018.06.058.

Teegavarapu, R. S. 2013. "Climate Change-Sensitive Hydrologic Design Under Uncertain Future Precipitation Extremes." *Water Resources Research* 49, no. 11: 7804–7814.

Thornthwaite, C. W., and J. R. Mather. 1955. "The Water Balance." *Publications in Climatology* 8, no. 1: 1–104.

Thornthwaite, C. W., and J. R. Mather. 1957. "Instructions and Tables for the Computing Potential Evapotranspiration and the Water Balance." *Publications in Climatology* 10, no. 3: 311.

Tonini, D. 1983. *Elementi di Idrografia e Idrologia*. Cortina.

Torrence, C., and G. P. Compo. 1998. "A Practical Guide to Wavelet Analysis." *Bulletin of the American Meteorological Society* 79, no. 1: 61–78. https://doi.org/10.1175/1520-0477(1998)079<0061:APGTWA>2.0.CO;2.

Trigo, R. M., T. J. Osborn, and J. M. Corte-Real. 2002. "The North Atlantic Oscillation Influence on Europe: Climate Impacts and Associated Physical Mechanisms." *Climate Research* 20: 9–17.

Tudoroiu, M., E. Eccel, N. Gioli, et al. 2016. "Negative Elevation-Dependent Warming Trend in the Eastern Alps." *Environmental Research Letters* 11, no. 4: 44021. https://doi.org/10.1088/1748-9326/11/4/044021.

von Weber Ebenhof, A. R. 1892. *Der Gebirgs-Wasserbau (Flussregulierung und Hauptschlucht-Verbauung) im alpinen Etsch-Becken und seine Beziehungen zum Flussbau des oberitalienischen Schwemmlandes*. Spielhagen und Schürich.

Wanner, H., S. Brrönnimann, C. Casty, et al. 2001. "North Atlantic Oscillation—Concepts and Studies." *Surveys in Geophysics* 22: 321–381.

WMO. 2010. *Manual of Streamgauging*. WMO.

Xiang, Y., C. Zeng, F. Zhang, and L. Wang. 2024. "Effects of Climate Change on Runoff in a Representative Himalayan Basin Assessed Through Optimal Integration of Multi-Source Precipitation Data."

10991085, 2025, 11, Downloaded from https://onlinelibrary.wiley.com/doi/10.1002/hyp.70305 by Fondazione Edmund Mach, Wiley Online Library on [03/11/2025]. See the Terms and Conditions (https://onlinelibrary.wiley.com/terms-and-conditions) on Wiley Online Library for rules of use; OA articles are governed by the applicable Creative Commons License

Journal of Hydrology: Regional Studies 53: 101828. https://doi.org/10.1016/j.ejrh.2024.101828.

Zampieri, M., E. Scoccimarro, S. Gualdi, and A. Navarra. 2015. "Observed Shift Towards Earlier Spring Discharge in the Main Alpine Rivers." *Science of the Total Environment* 503: 222–232. https://doi.org/10.1016/j.scitotenv.2014.06.036.

Zolezzi, G., A. Bellin, M. C. Bruno, B. Maiolini, and A. Siviglia. 2009. "Assessing Hydrological Alterations at Multiple Temporal Scales: Adige River, Italy." *Water Resources Research* 45, no. 12: W12421. https://doi.org/10.1029/2008WR007266.

Supporting Information

Additional supporting information can be found online in the Supporting Information section. **Appendix S1:** Supporting Information.

10991085, 2025, 11, Downloaded from https://onlinelibrary.wiley.com/doi/10.1002/hyp.70305 by Fondazione Edmund Mach, Wiley Online Library on [03/11/2025]. See the Terms and Conditions (https://onlinelibrary.wiley.com/terms-and-conditions) on Wiley Online Library for rules of use; OA articles are governed by the applicable Creative Commons License